2021 CIG Community Research Highlights

Preface

Founded in 2005 with support from the National Science Foundation, the Computational Infrastructure for Geodynamics (CIG) is an organization that supports the creation, development, and dissemination of the software that enables computational geodynamics and the formation, training, and mentoring of user communities. Through our actions we continue to transform the way the geodynamics communities view software and access computing creating both immense opportunities as well as challenges. These opportunities catalyze and drive research in geodynamics.

As we approach the next five years of CIG, we have reached out to the community to provide examples of the science CIG has and continues to enable. The one-page research highlights here provide us with a snapshot of the science activities of our community. These activities provide a signpost for the future that aids in defining the needs of the community and helps to guide the organization.

Research highlights are organized by code and authors.

I encourage you to avail yourself of this rare opportunity to take in the breadth of CIG research as presented in a single document.

Lorraine J. Hwang, editor

dynamo seismology computational science short term crustal dynamics CIG COMPUTATIONAL INFRASTRUCTURE for GEODYNAMICS mantle convection melt and volatiles long term tectonics education

CIG is funded under NSF-1550901

Table of Contents

ASPECT

CALYPSO

CITCOMS

PYLITH

SPECFEM2D

SPECFEM3D

SPECFEM3D CARTESIAN

SPECFEM3D GLOBE

SW4

Interaction between tectonics, erosion, and sedimentation during the formation of rifted continental margins

Sascha Brune, Derek Neuharth, Anne Glerum, Xiaoping Yuan, Jean Braun
GFZ Potsdam, Germany

Erosion and sedimentation at plate boundaries are known to be primarily affected by vertical tectonic motions. Conversely, the tectonic evolution of brittle and ductile crust depends on topographic surface loads that are in turn controlled by surface processes. We address this interaction by coupling the CIG geodynamics code ASPECT to the open-source surface process code FastScape (Yuan et al., 2019). Preliminary model results demonstrate the tight connection between normal fault longevity, block rotations, and sedimentation patterns. Marine sedimentation leads to prolonged delay in continental break-up and facilitates rift migration as well as formation of hyper-extended crust (Brune et al., 2014).

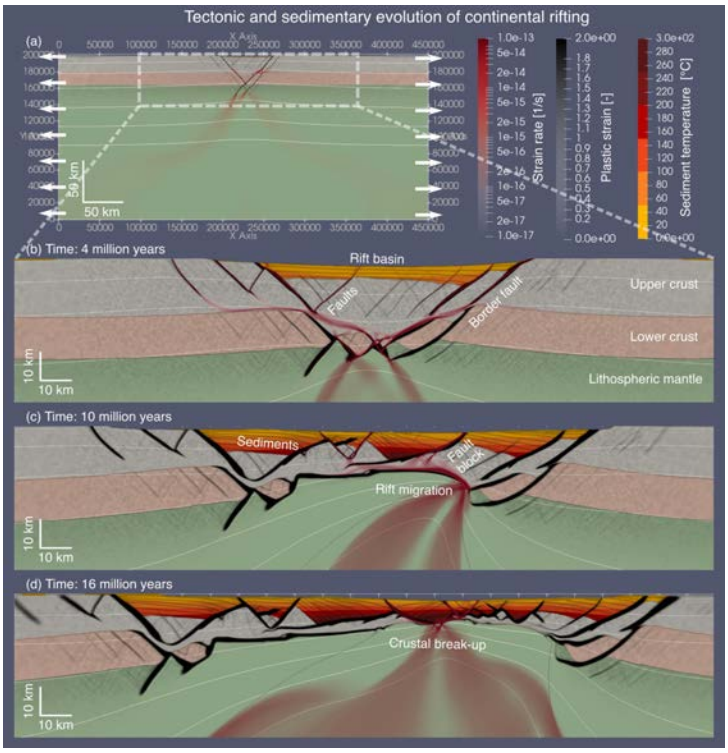

High-resolution 2D rift models of joint tectonic and sedimentary evolution from onset of rifting to final crustal break-up. Rifted margin asymmetry emerges spontaneously during fault network evolution. Active faults and shear zones are depicted in red, inactive ones in black. Sediments are colored in terms of their temperature (orange/red) and contoured in 1-million-year deposition intervals. These contours illustrate the tight connection between upper-crustal faults, rotation of normal fault blocks and the sedimentary structure. We exploit the mesh refinement capabilities of ASPECT by employing coarse (10 km) elements in the lower part of the model. Towards the surface and the model center, elements are successively refined 5 times to a minimum element size of 312.5 m. Given the second order elements, this results in an effective resolution of ~150 m.

CIG Code(s): ASPECT

References

Brune, S., Heine, C., Perez-Gussinye, M., & Sobolev, S. V. (2014). Rift migration explains continental margin asymmetry and crustal hyper-extension. *Nature Communications*, *5*(4014).

Yuan, X. P., Braun, J., Guerit, L., Simon, B., Bovy, B., Rouby, D., et al. (2019). Linking continental erosion to marine sediment transport and deposition: A new implicit and O(N) method for inverse analysis. *Earth and Planetary Science Letters*, *524*, 115728.

Teaching Introduction to Geophysics using ASPECT

Juliane Dannberg

I use the modeling software ASPECT, inside a virtual Linux environment that students install on their computers, to teach my class "Introduction to Geophysics". In my course, I discuss the structure and the motion of material in the Earth's interior. This includes answering questions such as: What is plate tectonics and what causes plates to move? What processes lead to volcanism and where is melt present in the Earth's interior? What are the major structures inside the Earth and what processes lead to the formation of these structures? In addition, I discuss the constraints on these problems provided by paleomagnetism, mineral physics, seismology, volcanology, geochemistry, petrology, and other disciplines.

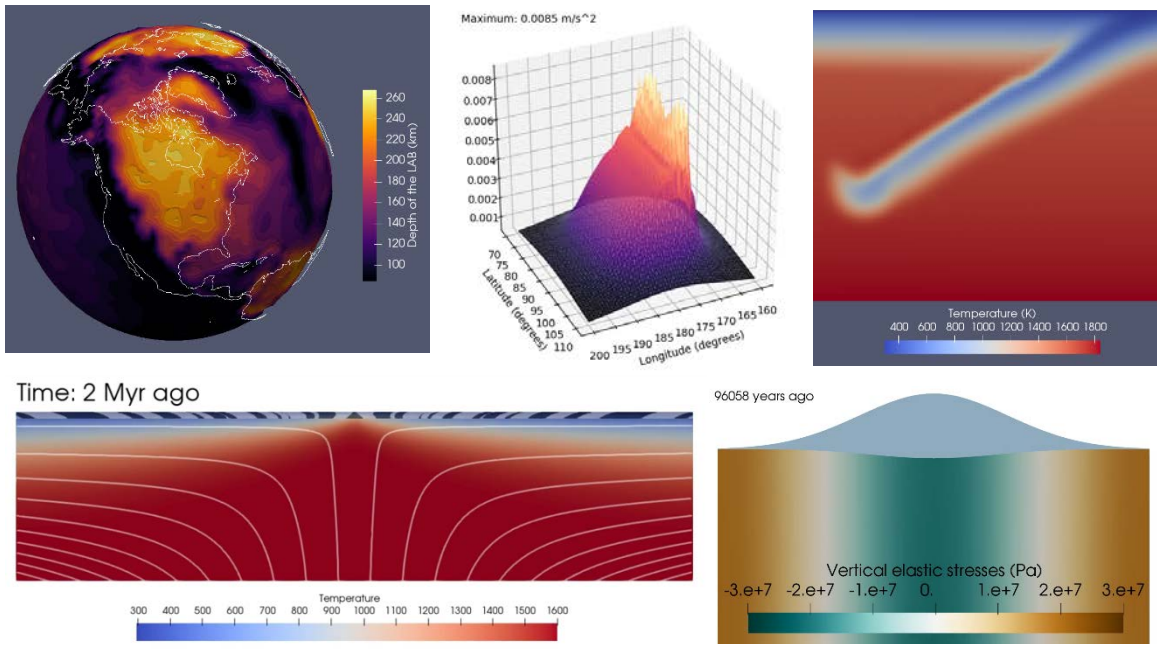

Examples of ASPECT applications used in my class: Model of lithospheric thickness (top left), the gravity anomaly above a dense slab (top cente), a subduction zone (top right), magnetic lineations at a mid-ocean ridge (bottom left), and the change in topography due to postglacial rebound (bottom right).

To teach these concepts, I use a variety of applications that can be modeled using ASPECT. This includes computing convective and conductive heat flux, the onset of convection, the spreading of plates at mid-ocean ridges, magnetic lineations at the seafloor, folding and faulting of crustal rocks, the break-up of plates, postglacial rebound, bending of plates caused by ocean islands, computing gravity anomalies, modeling subduction zones and mantle plumes, and post-orogenic collapse. Students run these models as examples in class and as part of homework assignments and are able to vary model parameters on their own to test their influence on the model results. Throughout the class, they learn not only geophysical concepts and quantitative skills, but also how to use a state-of-the-art geodynamic modeling software.

CIG Code(s): ASPECT

Modeling magma/mantle dynamics

Juliane Dannberg, Rene Gassmoeller, Timo Heister, Robert Myhill, Sanne Cottaar

Mantle melting and magma transport have been a subject of great interest in the geosciences for a long time, as they are directly related to volcanism. However, their vastly different timescales make it difficult to study mantle convection and melt migration in a unified framework, especially for 3-D global models. We have developed a new formulation of the equations for coupled magma/mantle dynamics that allows it to accurately compute large-scale 3-D magma/mantle dynamics simulations including large regions without melt. A key strategy for incorporating melt migration is the use of adaptive mesh refinement to increase resolution only in areas where melt is present.

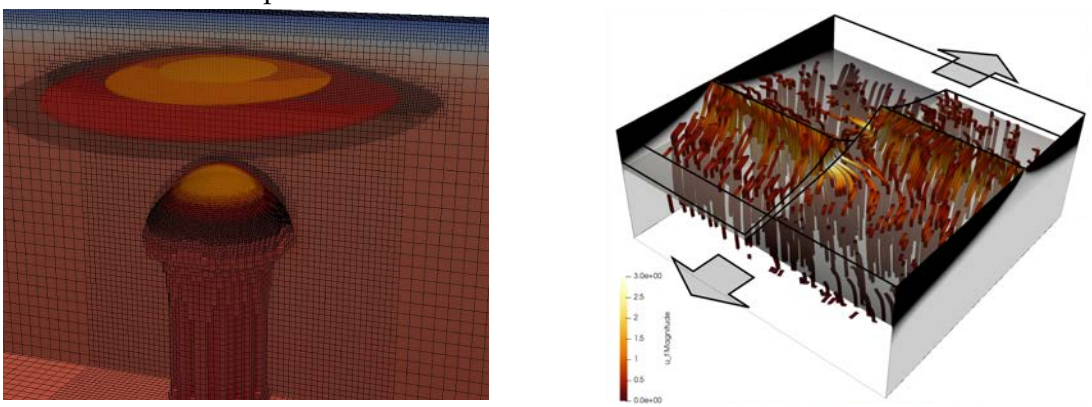

Magma dynamics in a plume (left, illustrating adaptive mesh refinement) and at a mid-ocean ridge with a transform fault (right), with streamlines illustrating the flow of melt.

We have applied this new formulation of magma/mantle dynamics to explore the hypothesis that present-day deep mantle melting creates observed zones of strongly reduced shear-wave velocity near the core-mantle boundary (so-called ULVZs). Our models explore the generation and migration of melt in a deforming and compacting host rock at the base of a plume in the lowermost mantle. Generally, we find partial melt alone does not explain the observed ULVZ morphologies and solid-state compositional variation is required to explain the anomalies. Our findings are an important step towards constraining the nature of the heterogeneities in the lowermost mantle and their influence on the thermal, compositional, and dynamical evolution of the Earth.

CIG Code(s): ASPECT

References

Dannberg, J., & Heister, T. (2016). Compressible magma/mantle dynamics: 3-D, adaptive simulations in ASPECT. Geophysical Journal International, 207(3), 1343-1366.

Dannberg, J., Gassmöller, R., Grove, R., & Heister, T. (2019). A new formulation for coupled magma/mantle dynamics. Geophysical Journal International, 219(1), 94-107.

Dannberg, J., Myhill, R., Gassmöller, R., & Cottaar, S. The morphology, evolution and seismic visibility of partial melt at the core-mantle boundary: Implications for ULVZs. Geophysical Journal International, submitted.

A possible origin of strike-slip faulting in an extending upper plate. The Aegean example.

Faucher, A.[1], Gueydan, F.[1], van Hunen, J.[2]
[1]Université de Montpellier, [2]Durham University

In the Mediterranean system, strike-slip faults are common inside upper extending plate of subduction zones with southward slab-roll back. Active since the Miocene times, numerous dextral strike-slip faults coexisted at this period with normal faults at the scale of the entire Aegean domain at the onset the westward Anatolia extrusion. Our objective is therefore to quantify if the combination of extension caused by slab-roll back and compression induced by Anatolian extrusion, intrinsically leads to the development of strike-slip faults. Here we show, using 3D modelling, that an extension coupled with a shortening orthogonal to it and at the same rate, can trigger strike-slip faulting in a hot deforming continental lithosphere. A 3D "Aegean-like" model in two deformation stages (first only extension and second equal shortening and extension) shows that several rifts form during the first stage of deformation that are, during the second deformation stage, rimmed by dextral and sinistral strike-slip faults. This suggests that the extension (slab-roll back) and shortening (Anatolian extrusion) can interact in space and time in the Aegean domain to create a complex tectonic pattern with coeval active normal faulting (e.g. Corinth and Evvia rifts) and dextral strike-slip faulting (e.g. Myrthes-Ikaria fault).

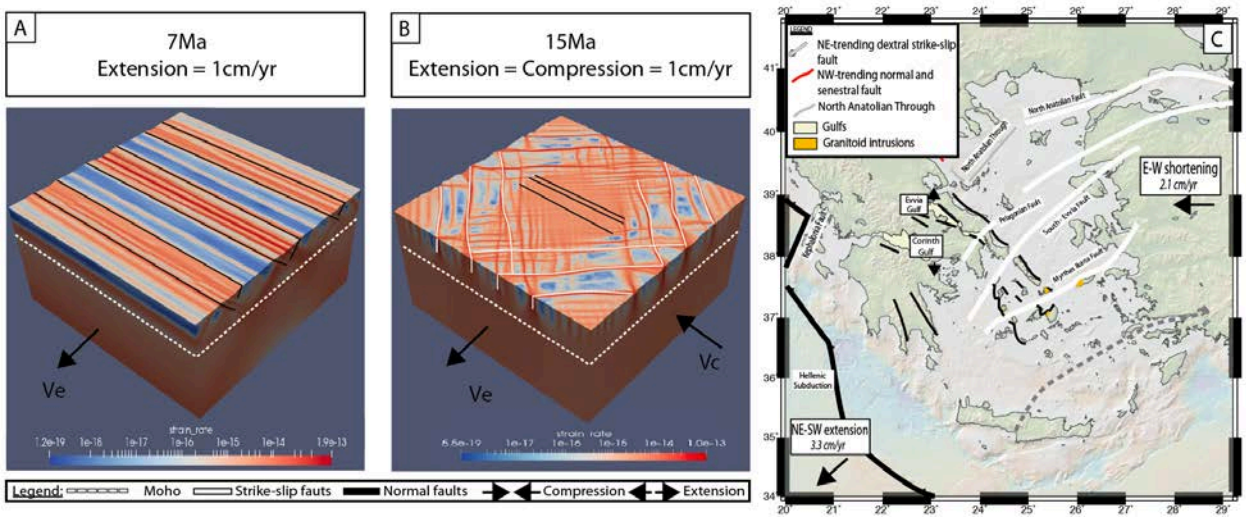

The "Aegean-like" 3D Model: Results shown after A/ 7 Ma (of only extension; Ve=1 cm/a), B/ 15 Ma (7.5 Ma of extension and 7.5 Ma of compression; Vc=Ve=1 cm/a), C/ Aegean map with normal faults rimed by strike-slip faults.

CIG Code(s): Advanced Solver for Problems in Earth's ConvecTion (ASPECT)

References

A. Faucher; F. Gueydan; J. van Hunen (2021). A possible origin of strike-slip faulting in an extending upper plate. The Aegean example. In prep.

Crystal Preferred Orientation in ASPECT

Menno R.T. Fraters and Magali I. Billen
UC Davis

Mantle flow causes grains to rotate into a preferred alignment, also called Crystal Preferred orientation, or CPO. Seismic anisotropy measurements can be used to determine this alignment of the grains. These seismic anisotropy measurements could therefore in theory be used to constrain mantle flow. The problem is that the link between mantle flow, CPO and seismic anisotropy is complicated. We have implemented a CPO model called D-Rex into the geodynamics code ASPECT. We show that the implementation yields valuable data which can be used to constrain models with seismic anisotropy measurements and is cheap enough to add to regular model runs.

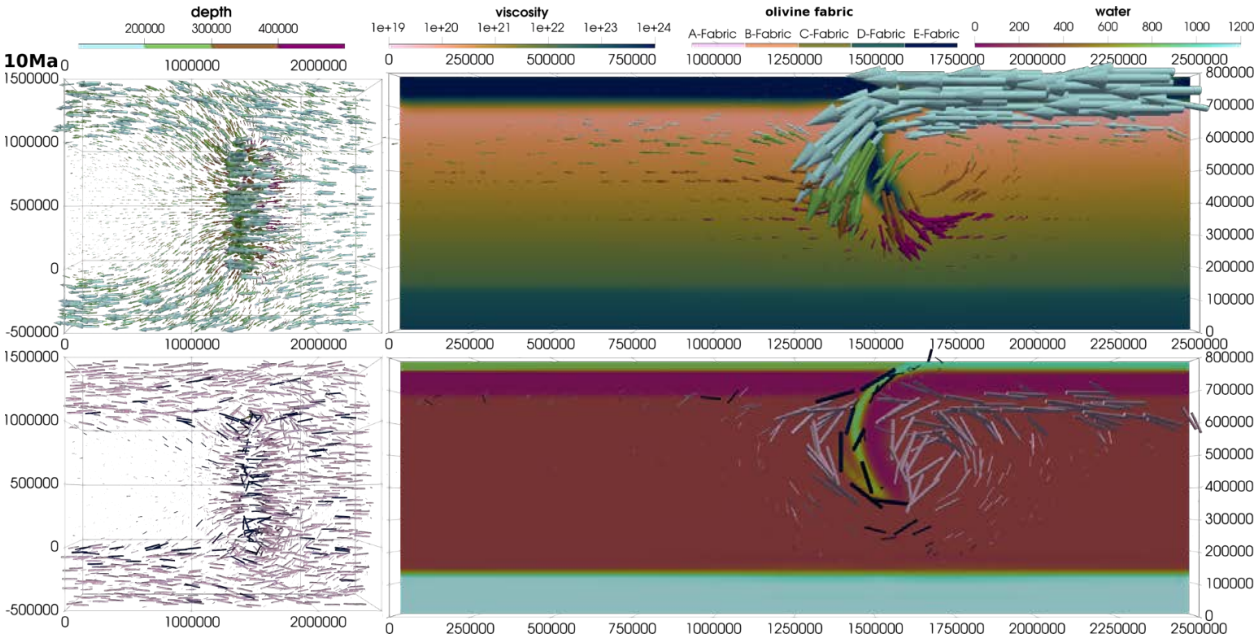

This image shows the velocity directions and magnitude (arrows) and viscosity fields in the top and the CPO directions (cylinders) and water content in the bottom for a simple 3D subduction model. The two pictures on the left are top views of the models, and the figures on the right are cross sections through the slab and overriding plate.

CIG Code(s): ASPECT

Acknowledgements: Wolfgang Bangerth, Rene Gassmöller and Hoayuan Li.

References

Fraters, M. R. T. and M. I. Billen, On the implementation and usability of CPO evolution in geodynamic modelling, Geochem. Geophys. Geosys., In prep.

The Geodynamic World Builder: a solution for complex initial conditions in numerical modeling

Menno Fraters[1,3], Cedric Thieulot[1], Arie van den Berg[1], and Wim Spakman[1,2]
[1] Department of Earth Sciences, Faculty of Geosciences, Utrecht University, Utrecht, the Netherlands, [2]Centre of Earth Evolution and Dynamics (CEED), University of Oslo, Oslo, Norway, [3] Department of Earth and Planetary Sciences, UC Davis, Davis, USA

The Geodynamic World Builder (GWB) is an open-source code library intended to set up initial conditions for computational geodynamic models in both Cartesian and spherical geometries. The inputs for the JSON-style parameter file are a structured nested list describing tectonic features, e.g., a continental, an oceanic or a subducting plate. Each of these tectonic features can be assigned a specific temperature profile (e.g., plate model), composition label (e.g., uniform) or a Crystal Preferred Orientation (CPO). For each point in space, the GWB can return the composition, temperature and/or CPO. It is written in C++ but can be used in almost any language through its C, Fortran and Python wrappers. The GWB has been tightly integrated with ASPECT and comes standard with the code. The creation of the GWB would not have been possible with the support of the Aspect community and CIG.

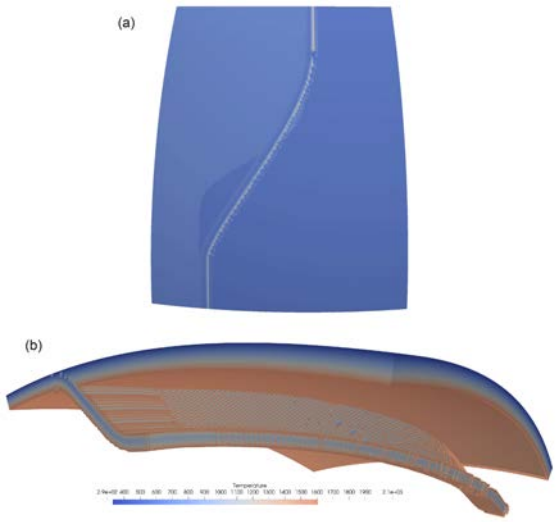

Images of a subduction geometry which can be easily set up in ASPECT with the GWB.

CIG Code(s): ASPECT

Acknowledgements: Timo Heister, Wolfgang Bangerth and Rene Gassmöller

References

Fraters, M., Thieulot, C., van den Berg, A., and Spakman, W.: The Geodynamic World Builder: a solution for complex initial conditions in numerical modeling, Solid Earth, 10, 1785–1807, https://doi.org/10.5194/se-10-1785-2019, 2019.

Massively-parallel matrix-free geometric Multigrid on adaptively refined meshes for Stokes flow

Timo Heister and Thomas C. Clevenger
Clemson University

The simulation of mantle convection requires the solution of a Stokes system to compute velocity and pressure variables. Solving this linear system accurately is challenging because of the large number of unknowns required, even with adaptive mesh refinement, and the large changes in viscosity throughout the domain. To answer important science questions regarding the history of our planet, highly accurate simulations require algorithms that scale to 100 million unknowns on the largest machines.

Like many other mantle convection codes, ASPECT relied on a matrix-based algebraic multigrid method for the Stokes system, that uses 80% or more of the runtime and most of the memory to store the system matrix for typical computations. Scalability is deteriorating above 10,000 cores and 10s of million of unknowns.

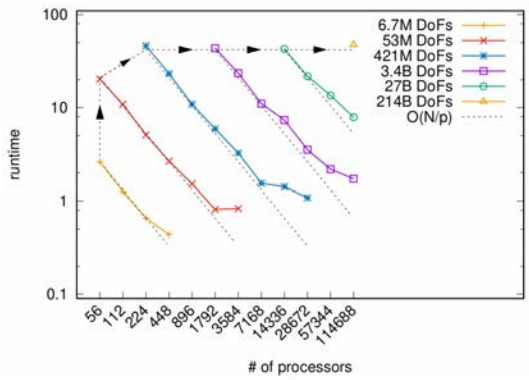

Strong and weak scaling from [Clevenger 2021] on TACC Frontera for a single Stokes solve with up to 214 billion unknowns.

As part of CIG, we developed a novel matrix-free (no system matrix storage), geometric multigrid method with novel parallel partitioning for highly scalable computations (Clevenger et al 2020). This has been implemented in the finite element library deal.II, on which ASPECT is built. We then ported the solver in ASPECT (Clevenger 2021) and show great scalability up to 114k MPI ranks (on TACC Frontera) with 200 billion unknowns. Simulations are more robust, 3x faster, and require 14x less memory.

CIG Code(s): ASPECT

References

Thomas C. Clevenger, Timo Heister, Comparison Between Algebraic and Matrix-free Geometric Multigrid for a Stokes Problem on an Adaptive Mesh with Variable Viscosity. Numerical Linear Algebra with Applications, 2021. https://doi.org/10.1002/nla.2375

Thomas C. Clevenger, Timo Heister, Guido Kanschat, Martin Kronbichler, A Flexible, Parallel, Adaptive Geometric Multigrid Method for FEM. ACM Trans. Math. Softw. 47, 1, Article 7 (December 2020).

Sea level indicators atop a slab window in southern Argentina—using geodynamic models to understand subduction behavior, its imprint on Earth's surface, and implications for Pliocene sea level

Andrew Hollyday[1], Jacqueline Austermann[1], Andrew Lloyd[1], Mark Hoggard[1,2], Fred Richards[3], Alessio Rovere[4]

[1]Columbia University & Lamont-Doherty Earth Observatory, [2]Harvard University, [3]Imperial College London, [4]University of Bremen

The effect of dynamic topography change on paleo-shoreline deposits is among the greatest sources of uncertainty in computing how high sea level was in the past. We use ASPECT to model mantle convection and dynamic topography through time to correct the elevations of three shorelines dated to the early Pliocene in southern Argentina (see Figure). Our models are constrained by global and local seismic tomography-derived structures, including the Patagonian slab window from the ANT-20 regional adjoint tomography model (Lloyd et al., 2020). We perform a suite of convection simulations varying the temperature and viscosity input as well as surface plate motions to identify the simulation that best fits the observed surface deformation. We correct the elevations of paleo sea level using the subset of models that fit the spatial uplift trends and further correct the data for glacial isostatic adjustment. This enables us to infer global mean sea level during the early Pliocene, a period when CO_2 and temperatures were higher than today.

A	65 - 75 m	5.15 ± 0.35 Ma
B	170 - 185 m	5.1 ± 0.30 Ma
C	34.5 - 38.9 m	4.98 ± 0.23 Ma

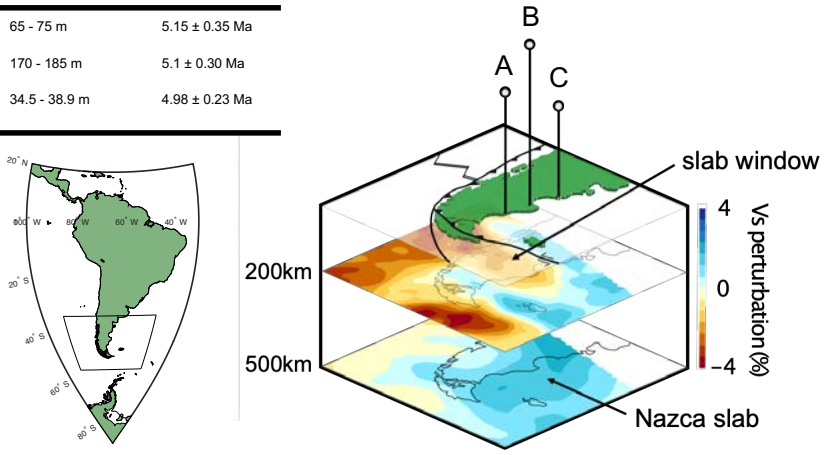

Seismic velocities at 200 km and 500 km depths from the Patagonian slab window (right; Lloyd et al., 2020) underlying three early Pliocene shorelines that have been uplifted by change in dynamic topography over the last 5 Ma (sites A, B, C). Table shows the present-day elevations of the sea level indicators and their ages.

CIG Code(s): ASPECT

References

Lloyd, A.J., et al. Seismic Structure of the Antarctic Upper Mantle Imaged with Adjoint Tomography. J. Geophys. Res.: Solid Earth (2020)

Origin of Intraplate Earthquakes in the Korean Peninsula: Insights from Tomography-Based Stress Models

Lee S.[1], Saxena A.[2,3], Song J.-H.[1], Rhie J.[1] and Choi E.[2]
[1]Seoul National University, [2]University of Memphis, [3]University of Florida

The origin of the stresses responsible for seismicity in the Korean Peninsula (KP) has been subject to much debate. Since the importance of lateral lithospheric thickness variations has been identified in previous studies, we assess contributions to this region's stress field from crustal and upper-mantle heterogeneities. We created numerical models using ASPECT, an open-source geodynamic modeling code. Our models include variations in this region's crustal thickness and heterogeneities in the upper mantle, which were inferred from seismic tomography. We show that the stress field generated by the upper mantle heterogeneities and east-west regional compression is quantitatively consistent with the KP's seismicity, along with other geophysical constraints such as surface topography and orientation of maximum horizontal stress. Furthermore, we suggest a novel perspective to the diffuse seismicity of the KP that the earthquakes in the west and those along the eastern coast of the KP may have different origins: the rim-of-craton effect and the mantle upwelling, respectively.

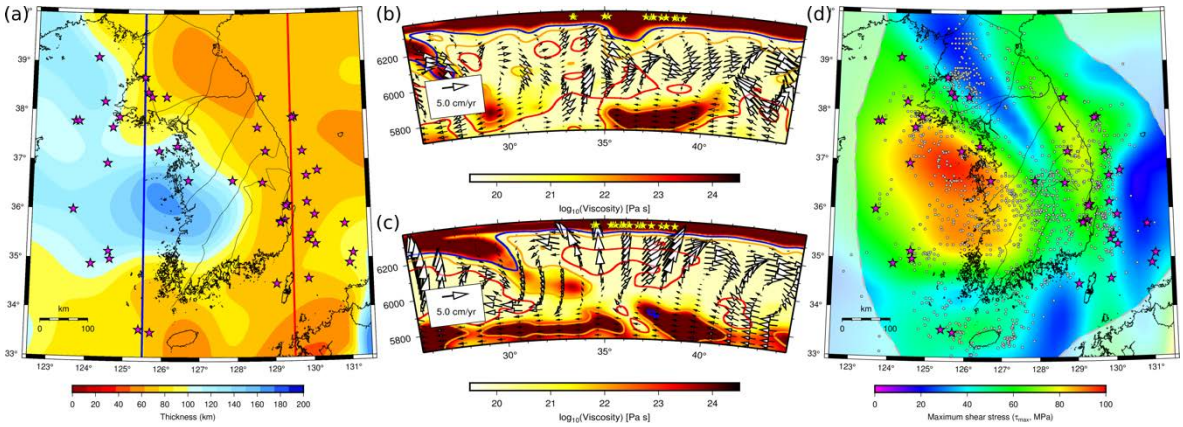

Images of (a) inferred lithospheric thickness with the 1300 K isotherm, spatial distribution of the velocity, temperature anomalies, and viscosity on cross-sections (b) along with blue line and (c) along with red line, (d) Spatial distribution of vertical averaged (surface to 20 km depth) maximum shear stress. In top view, events greater than M_L 3.0 and M_L 4.0 are indicated by white dots and magenta stars, respectively. Blue, orange, red, dark red contours represent the temperature at 1300 K, 1600 K, and 1900 K, respectively. Yellow stars in panels (b) – (c) indicate epicenters which are ±1° adjacent to the cross-sections and greater than M_L 4.0.

CIG Code(s): ASPECT

References

Lee, A., Saxena, A., Song, J.-H., Rhie, J., and Choi, E., Origin of seismicity in the Korean Peninsula and implications for intraplate earthquakes, (under review).

The origin of the Cameroon Volcanic Line.

Matthew D. C. Likely[1], Jeroen van Hunen[1], Linda Kirstein[2], Godfrey Fitton[2], Lara Kalnins[2], Jenny Jenkins[1], & Ana Negredo[3]
[1]Department of Earth Sciences, Durham University, [2]School of GeoSciences, Edinburgh University, [3]Department of Earth Physics and Astrophysics, Universidad Complutense, Madrid

The origin of intraplate volcanism remains strongly debated, with mantle plumes being the dominant explanation for such volcanism. However, not all examples possess the characteristics displayed by plume volcanic chains, such as age progression, OIB geochemistry and a potential deep-seated thermal anomaly. Here, we utilise ASPECT to produce numerical models to investigate the magmatism along the Cameroon Volcanic Line. Convection is triggered where there is a large lithospheric thickness gradient and the presence of small-scale convection which form as a result of lithospheric instabilities [King and Anderson, 1998]. We explore how this plate-mantle interaction, combined with mobilized metasomatized sub-continental mantle lithosphere, might explain the local intraplate magmatism [Priestley *et al.*, 2019].

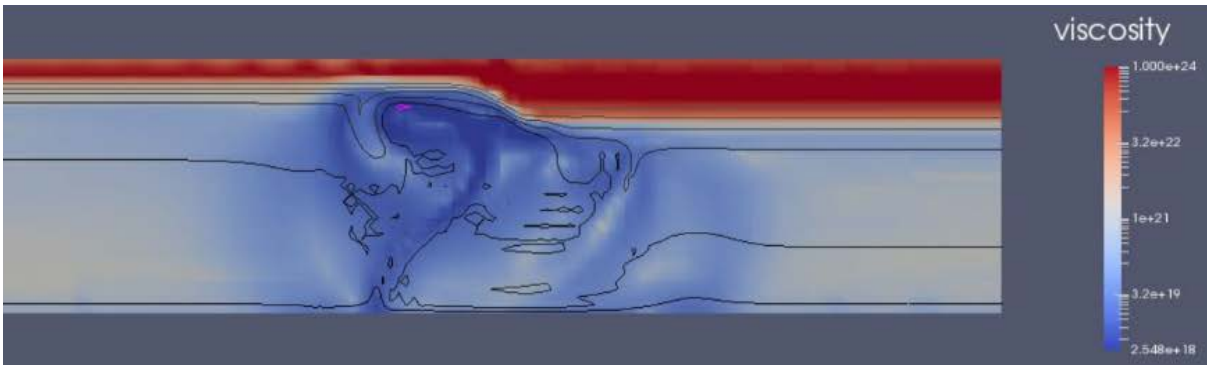

A model in the process of convection, with a cool downwelling, inducing a warmer upwelling of material. The pink signature is the presence of melt from both decompression and a reduction in the local solidus via the fertile material initially below the craton.

CIG Code(s): ASPECT

References

King, S. D. & Anderson, D. L. (1998), Edge-driven convection. *Earth and Planetary Science Letters*, **160**(3-4), 289-296, doi:10.1016/S0012-821X(98)00089-2.

Priestley. K., McKenzie, D. & Ho, T. (2019), A Lithosphere-Asthenosphere Boundary – a Global Model Derived from Multimode Surface-Wave Tomography and Petrology. *Lithospheric Discontinuities. AGU Geophysical Monograph* **239,** 111-123, doi:10.1002/9781119249740.ch6

Thermo-mechanical modelling of subducting plate delamination in the northern Apennines.

Ana M. Negredo[1], Carlos Clemente[1], Eugenio Carminati[2], Ivone Jiménez-Munt[3], Jaume Vergés[3], Javier Fullea[1], Montserrat Torné[3]

[1]Complutense University of Madrid, [2]University of Rome La Sapienza, [3]Geosciences Barcelona

A number of previous studies indicate the possibility of post-collisional continental delamination in the northern Apennines. In this study we used ASPECT code to investigate by means of thermo-mechanical modelling the conditions for, and consequences of, delamination postdating continental subduction in this region. The initial model setup simulates the scenario at ca 20 Ma, where the oceanic lithosphere of the westward-subducting Adria plate was entirely consumed and some amount of continental subduction also occurred. Consistent with geological data, the compressional front produced by delamination migrates about 260 km eastwards, causing a similar migrating pattern of extension. The topographic response is computed by means of a true free-surface approach, and reflects the same eastward migrating pattern of uplift caused by asthenospheric inflow in the internal part of the system and crustal thickening; and subsidence at the front caused by the negative buoyancy of the sinking Adria slab. The conditions for the occurrence of magmatism and high heat flow beneath Tuscany are also explored.

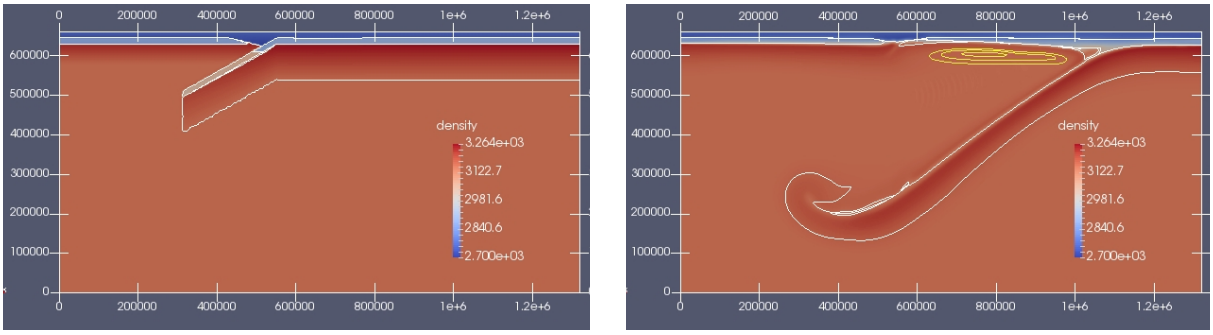

Images of the ASPECT simulation showing (left) the initial setup and (right) the mass redistribution after 20 Myr of evolution. The lithospheric mantle delaminates from the crust and rolls back eastwards. The yellow isolines show melt fractions of 4%, 8% and 12%.

CIG Code(s): ASPECT and deal.ii

Acknowledgements: The present research has been funded by the Spanish Ministry of Science and the Madrid Region.

References

Negredo, A. M, C. Clemente, E. Carminati, I. Jiménez-Munt, J. Vergés, J. Fullea, M. Torné, Thermo-mechanical modelling of subducting plate delamination in the northern Apennines. In preparation.

Geodynamic Modelling of Incipient Edge-Delamination in the Central Betic orogen (south Spain).

Ana M. Negredo[1], Flor de Lis Mancilla[2], Carlos Clemente[1], Jose Morales[2] and Javier Fullea[1]
[1]Complutense University of Madrid, [2]University of Granada

Such tearing is often accommodated via subvertical STEP (Subduction-Transform Edge Propagator) faults that cut across the entire lithosphere resulting in sharp lateral thermal and rheological variations across the juxtaposed lithospheres. This setting favors the occurrence of continental delamination. In this study, we used the code ASPECT to investigate by means of thermo-mechanical modelling the conditions for, and consequences of, delamination associated with STEP faults without imposing any ad hoc forcing. We assumed a viscoplastic rheology based on the combination of plastic and composite viscosities. ASPECT has two particular advantages for modeling continental delamination: the adaptive mesh refinement (AMR), which allows for selective mesh refinement in areas of strong gradients in the material properties, and the incorporation of free surface on the top boundary, which allows for self-consistent modelling of the surface response to mass redistribution during delamination.

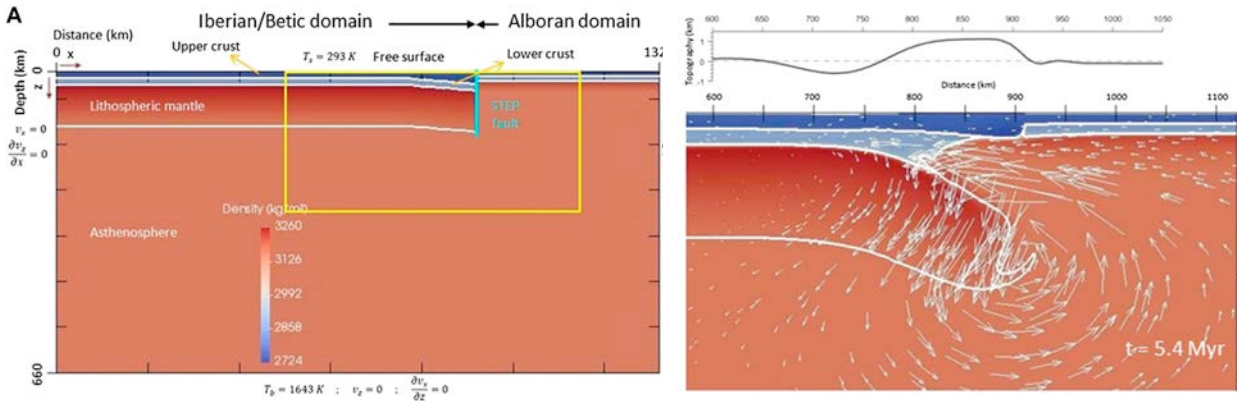

Initial setup and boundary conditions (left) after slab detachment via a STEP fault. Mass distribution, velocity field, and topographic response (top right) to incipient lithospheric mantle peeling and asthenospheric inflow.

CIG Code(s): ASPECT and deal.ii

Acknowledgements: The present research has been funded by the Spanish Ministry of Science and the Madrid Region

References

Negredo, A. M, FdL. Mancilla, C. Clemente, J. Morales and J. Fullea, Geodynamic modelling of edge-delamination driven by STEP faults: the westernmost Mediterranean margin (central Betic orogen) case study, Frontiers in Earth Science, 2020, (8), 435. doi:10.3389/feart.2020.533392.

On the Educational Uses of ASPECT.

Ana M. Negredo, Juan Rodríguez-González, Javier Fullea
Complutense University of Madrid

Open-source, free and well-documented codes like ASPECT offer invaluable advantages for education uses. In the degree of Physics and in the Master of Geophysics and Meteorology of the Complutense University of Madrid, we have gained a wide experience in supervising both undergraduate and Master thesis projects, as well as in short geodynamics exercises performed in the computing laboratory. Due to funding limitations, these activities would not be feasible with commercial software. Students that are to use ASPECT have previous basic knowledge on geodynamic processes, numerical methods, programming language and Linux operating system. In the following we present a typical training plan and some examples of recent research projects. i) The student is provided with the basic literature about the geodynamic process to be modelled, ii) she/he has develop the governing equations from the primitive forms (basic equations of conservation of mass, momentum and energy), including the different approximations, iii) after downloading and installing ASPECT (optional) students perform a number of tests by running and modifying selected cookbooks; reading of several sections of ASPECT user's manual is needed in this stage; results are plotted with the open source visualization application Paraview, iv) with the help of the supervisor, the student creates the input parameter file and usually performs a complete parametric study. Students are finally trained on scientific communication since they have to write a 25 pages dissertation and perform an oral presentation.

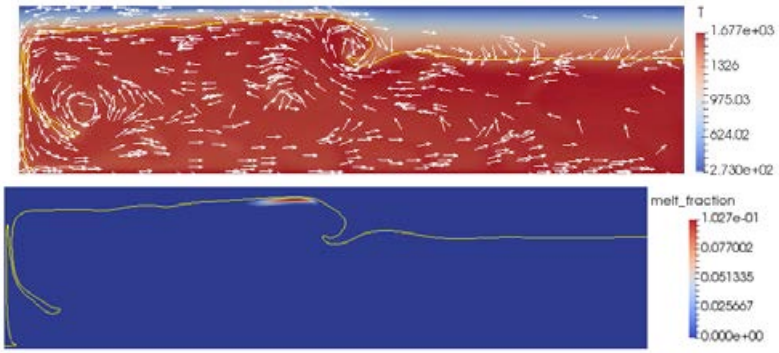

Images of the ASPECT simulation of edge-driven convection showing (top) the temperature and velocity field and (bottom) generated melt fraction adjacent to the craton edge. Figures from Cecilia Albizúa Master thesis project.

Different examples of ASPECT applications in educational projects include modelling of edge driven convection, both to study the generic process and its application to the Antarctic plate; modelling of continental delamination; modelling of slab breakoff and its topographic response.

CIG Code(s): ASPECT and deal.ii

Thermo-Mechanical Modelling to Unravel the Origin of the Canary Islands.

Ana M. Negredo[1], Jeroen van Hunen[2], Juan Rodríguez-González[1] and Javier Fullea[1]
[1]Complutense University of Madrid, [2]Durham University

The complex structure and geodynamic setting of the Canary Islands has led to different hypotheses about its origin and evolution, which is still a matter of a vivid debate. In addition to the classic mantle plume hypothesis, a mechanism of small-scale mantle convection at the edge of cratons (Edge Driven Convection, EDC) has been proposed. A combination of mantle plume upwelling and EDC has also been hypothesized. In this study we evaluated these hypotheses quantitatively by means of numerical thermo-mechanical models using ASPECT code. We assumed a composition- and temperature-dependent viscosity. Given that ASPECT is a very well documented and open code we were able to create a new 'material model' extension to estimate the amount of melt by means of the 'passive advection approach' described by Gassmöller et al. (2016; see their supplementary information).

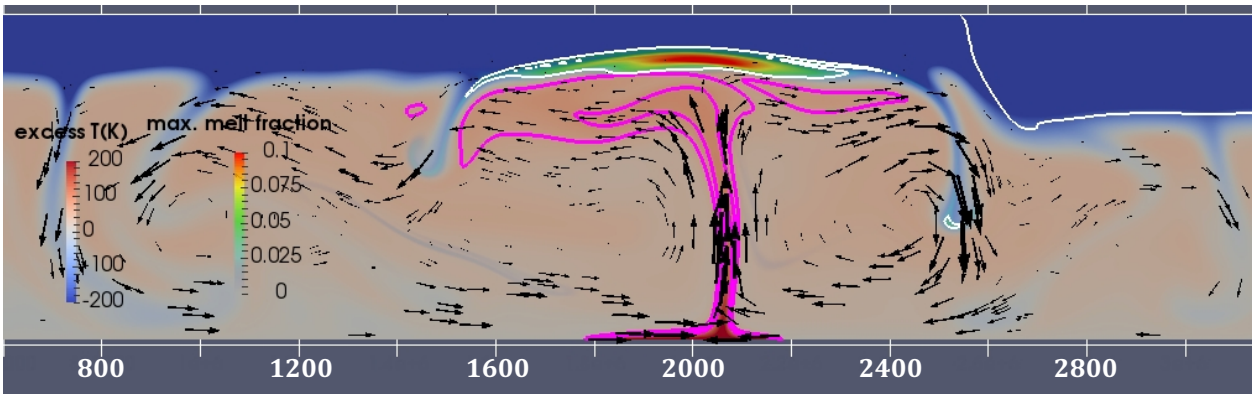

Velocity field, melt fraction and temperature excess distribution for a simulation combining EDC and upper mantle plume upwelling. White contours outline the region with maximum melt fraction > 0.03 (3%). Pink lines show the 50, 75 and 100 K temperature excess isolines.

CIG Code(s): ASPECT and deal.ii

Acknowledgements: The present research has been funded by the Spanish Ministry of Science and the UK Natural and Environmental Research Council.

References

Negredo, A. M, J. van Hunen, J. Rodríguez-González and J. Fullea, On the Origin of the Canary Islands: Insights from mantle convection modelling, In prep.

Gassmöller, R., J. Dannberg, E. Bredow, B. Steinberger, and T. H. Torsvik, Major influence of plume-ridge interaction, lithosphere thickness variations, and global mantle flow on hotspot volcanism-The example of Tristan, Geochem. Geophys. Geosyst., 2016 (17), 1454–1479, doi:10.1002/2015GC006177.

Lithospheric Structure of the Malawi Rift: Implications for Magma-Poor Rifting Processes

Emmanuel A. Njinju[1], Estella A. Atekwana[2], D. Sarah Stamps[1], Mohamed G. Abdelsalam[3], Eliot A. Atekwana[2], Kevin L. Mickus[4], Stewart Fishwick[5], Folarin Kolawole[6], Tahiry A. Rajaonarison[1], Victor N. Nyalugwe[2]

[1]Virginia Tech, [2]University of Delaware, [3]Oklahoma State University, [4]Missouri State University, [5]University of Leicester, [6]University of Oklahoma

To better understand magma-poor rifting processes, we first derive lithospheric structure beneath the Malawi Rift, a segment of the magma-poor Western Branch of the East African Rift, from spectral analysis of Bouguer gravity anomalies of the World Gravity Model 2012. Second, we use ASPECT (Advanced Solver for Problems in Earth's ConvecTion) to investigate lithosphere-asthenosphere coupling beneath the Malawi Rift by using the new lithospheric structure as a constraint to develop a 3D numerical model of lithospheric modulated convection. We assume a viscoplastic rheology for the crust, dislocation creep for the lithospheric mantle, and diffusion creep for the sublithospheric mantle. We propose coupled extension beneath the rift's magmatic zones is magma-assisted, whereas decoupled extension beneath the magma-poor segments is assisted by a concentration of fluids, possibly fed from deeper asthenospheric melt that is yet to breach the surface.

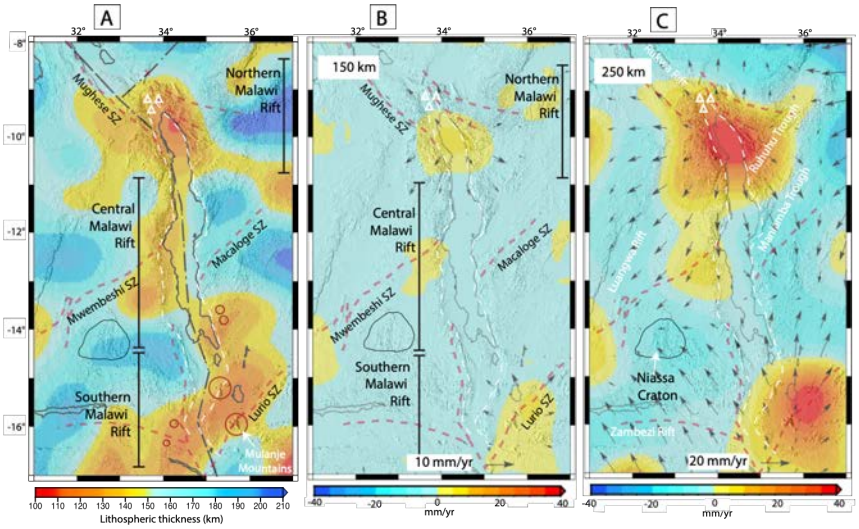

(A) Map of lithospheric thickness of the region. Red dashed lines show shear zones (SZ). Red circles show Ring-Complexes. Dashed black lines show plate boundaries from Stamps et al. [2008]. Modeled vertical velocities are overlain by horizontal velocities (black arrows). (B) Deformation of the lithospheric mantle at 150 km depth. (C) Lithospheric modulated convection of the asthenosphere at 250 km depth. White triangles represent volcanoes.

CIG Code(s): ASPECT

Acknowledgements: This modeling component of this work was funded by NSF EarthCube grant 1740704.

References

Njinju, E. A., Atekwana, E. A., Stamps, D. S., Abdelsalam, M. G., Atekwana, E. A., Mickus, K. L., Fishwick, S., Kolawole, F., Rajaonarison, T., Nyalugwe, V. N. (2019). Lithospheric Structure of the Malawi Rift: Implications for Magma-Poor Rifting Processes. Tectonics, 38(11), 3835-3853.

Gravity fields and their derivatives obtained with Newton integrals on a hollow sphere

C. Thieulot[1], L. Jeanniot[1], B. Root[2], J. Naliboff[3]
[1]Utrecht University, The Netherlands, [2]Delft University, The Netherlands, [3]New Mexico Institute of Mining, USA

The mass-density distribution of the Earth drives mantle convection and plate tectonics but remains uncertain. This mass distribution is responsible for the gravity field perceived by satellites such as GRACE and GOCE and such measurements can be used as a constraint on Earth models.

We have therefore implemented gravity field and gravity potential field calculations in the ASPECT code. These are based on the existing hexahedral tesselation of the planet (without the core) generated by the code and makes use of the Gauss-Legendre quadrature scheme which is part of the standard Finite Element methodology, albeit with an increased number of sample points for increased accuracy.

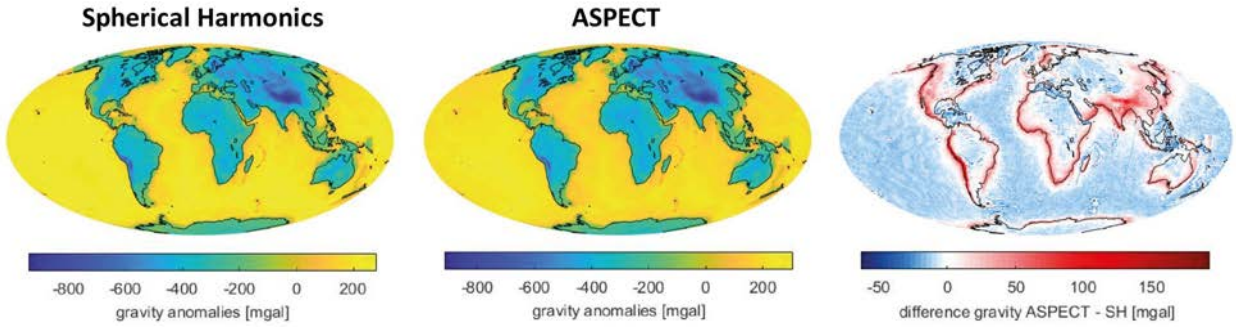

"Moho benchmark". The moho depth is given by the CRUST1.0 data set. Mantle material below it is given a constant density of 450kg/m^3 while the crustal material above it has been entirely removed. Comparison of results obtained with a spherical harmonics-based code (left), and ASPECT.

CIG Code(s): ASPECT

References

Jeanniot, Thieulot, Root, Naliboff, Spakman. On the accuracy of gravity fields and their derivatives obtained with Newton integrals on a hollow sphere tessellated with hexahedra, In prep.

Did mantle plumes contribute to early lithosphere formation?

Jeroen van Hunen[1], Graham Pearson[2], Lawrence H. Wang[3], Adam Welsh[1]
[1]Durham University, UK, [2]University of Alberta, Canada, [3]Institute for Energy Technology, Norway

Cratons, the oldest, thickest, most robust, and tectonically most inactive parts of the continents we live on, have survived billions of years of mantle convection and plate tectonics. The clue might be in their formation mechanism, but unfortunately, there is still significant debate over how these cratons formed. Multiple mechanisms have been proposed (e.g. Lee et al., 2011), and each mechanisms has its pros and cons, and are not mutually exclusive. One of those proposed mechanisms is the episodic addition of continental mantle roots by mantle plumes. While the geochemical arguments for the necessary conditions of such model have been extensively discussed (e.g. Wittig & Pearson, 2008), the dynamics of such mechanism remains largely unexplored. In this project, geodynamical modelling of this phenomenon is performed using the CIG ASPECT code, which offers many essential built-in features, such as adaptive mesh refinement to allow for large-scale 3-D models with sufficient local resolution, complex and realistic rheologies, and tracking of melting events. Preliminary results show that dehydration strengthening of the melting residue has to play an essential role if mantle plumes were (partly) responsible for the formation of cratons.

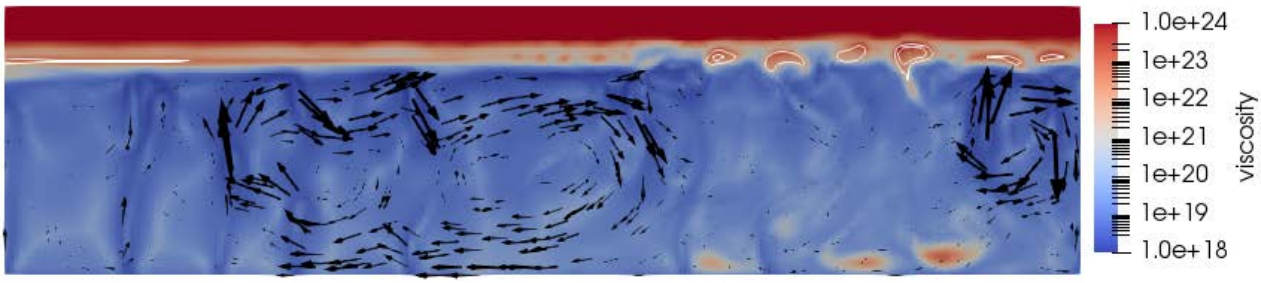

Simulation showing interaction between mantle plumes in a hotter, early Earth mantle and the lithosphere above. Preliminary 2-D upper mantle modelling illustrates how dehydration strengthening (white contours) of mantle plume melting residues in the asthenosphere increases viscosity (colours) locally and episodically to form additional mantle lithosphere.

CIG Code(s): ASPECT

References

Lee, C. T. A., Luffi, P. & Chin, E. J. in *Annual Review of Earth and Planetary Sciences, Vol 39* Vol. 39 *Annual Review of Earth and Planetary Sciences* (eds R. Jeanloz & K. H. Freeman) 59-90 (2011).

Pearson, D. G. & Wittig, N. Formation of Archaean continental lithosphere and its diamonds: the root of the problem. *Journal of the Geological Society* **165**, 895-914, doi:10.1144/0016-76492008-003 (2008).

Parallel Vector Visualization Using 3D Line Integral Convolution for Geodynamo Simulations

Yangguang Liao, Hiroaki Matsui, Oliver Kreylos, Magali Billien
University of California, Davis

It is widely accepted that the geomagnetic field is driven by the flow motion of the liquid iron alloy of the outer core. Numerical simulations have had large role for understanding the dynamics of the flow and dynamo processes. In geodynamo simulations, a three-dimensional model and extremely fine spatial resolutions are required to perform dynamo simulations to represent the turbulent in the outer core. Consequently, massively parallel computation is required for these geodynamo simulations in which visualization of these large, four-dimensional (time and space) data sets is a big challenge.

We developed a flow visualization system for a vector field on large unstructured grids using parallel 3D line integral convolution (LIC). To perform the simulation and visualization concurrently (so called *in-situ* visualization), the present LIC operation and rendering is performed for subdomains on each MPI process. The key issue for the parallel LIC visualization is that the balancing the computational costs among MPI processes. We introduce a load-balancing scheme based on estimated LIC computation time. After the re-partitioing of the spherical shell, the present model leads to more balanced computation and improved scalability than the original subdomains which is used for the simulation. We also compare the parallel scalability of the present LIC with the traditional integral field lines methods. LIC maintains good scaling up to 6144 processor cores while field line tracing keeps scaling up to 384 processor cores (See Figure).

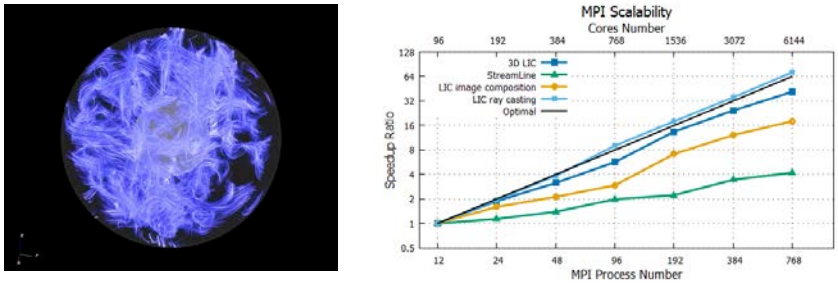

Direction of the magnetic field line in a rotating spherical shell modeled on the Earth's outer core visualized by the present LIC module (left). The magnetic field in the shell is dipolar dominated and is twisted by the columnar flow in the outside of the tangent cylinder. The speeding up of the LIC on TACC stampede 2 up to 6144 processor cores are plotted in the right.

CIG Code(s): Modified version from Calypso V.1.2

References

Liao, Y., H. Matsui, O. Kreylos, and L.H. Kellogg, Scalable Parallel Flow Visualization Using 3D Line Integral Convolution for Large Scale Unstructured Simulation Data, Eurographics Symposium on Parallel Graphics and Visualization, 2019, 20—25.

Temperature variation at the inner and outer core boundaries generated by the meridional circulation in the numerical dynamos

Hiroaki Matsui
University of California, Davis

Resent seismic observations suggests that inner core is seismically anisotropic. These studies suggest aspherical growth of the inner core. Slow viscous deformation of the inner core and latent heat distribution by flow motion are expected to be the origin of the aspherical growth of the inner core. To explain inner core anisotropy and aspherical growth of the inner core, a number of dynamo simulations have been performed with prescribed boundary conditions at the Inner Core Boundary (ICB) to take into account the inner core heterogeneity. In the present study, geodynamo simulations are performed with considering the heat equation throughout the inner and outer core in order to represent thermal structure of the ICB self-consistently.

The results show that the time averaged thermal structure at the ICB is likely to the simulation results with homogeneous heat flux boundary conditions. The time averaged temperature variation is approximately 26% of the average temperature difference between the ICB and Core-Mantle Boundary (CMB), while heat flux variation is only 6% of the average heat flux at the ICB. This temperature variation at ICB also generates high temperature region at both poles on the CMB and generate weak magnetic field region at the pole (see left and middle panels of the Figure). This high temperature region is only seen the dynamo case and increases with the Rayleigh number (see right panel of Figure). Looking at the force balance, balance of the Coriolis force and

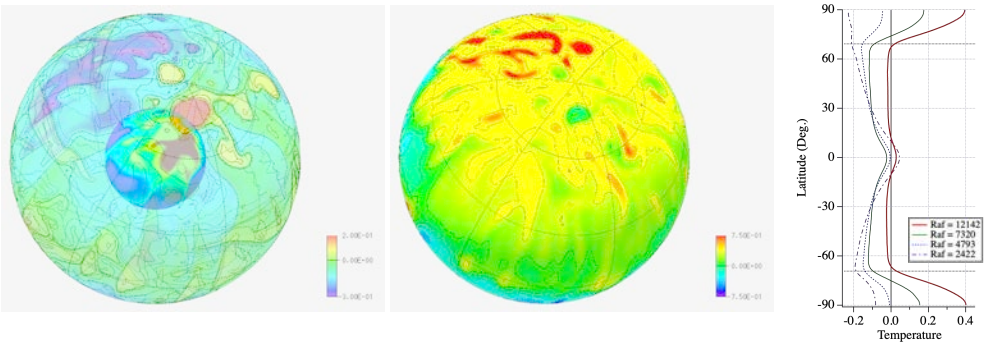

Lorentz force sustains the meridional circulation inside of the tangent cylinder.

Temperature at the ICB and CMB in the present dynamo simulation (left) and radial magnetic field at the CMB (middle). High temperature area is generated around the pole at both ICB and CMB, and the hot area at the CMB corresponds to the area with weak radial magnetic field. The time and zonal mean of the temperature at the CMB as a function of the latitude is plotted on the right. The high temperature area at pole is only generated in the dynamo cases and increases with the Rayleigh number.

CIG Code(s): Modified version from Calypso V.1.2

References

H. Matsui, Temperature variation at the inner and outer core boundaries generated by the meridional circulation in the numerical dynamos, in prep.

Investigation of Dipolar Dominancy in Geodynamo Simulations with Different Inner Core Sizes

Y. Nishida[1], Y. Katoh[1], H. Matsui[2], M. Matsushima[3], T. Kera[1], and A. Kumamoto[1]
[1]Tohoku University, [2]University of California, Davis, [3]Tokyo Institute of Technology

The solid inner core of the Earth has been growing for approximately one billion years due to the cooling of the Earth. The changing spherical shell geometry of the Earth's core is likely to have an influence on the geodynamo driven by convective motions in the fluid outer core. To understand the geometry effect on the dynamo regime through evolution of the core, we perform numerical simulations of geodynamo with three spherical shell radius ratios: r_i/r_o = 0.15, 0.25 and, 0.35, where r_i and r_o are the inner and outer core radii, respectively. In the present study, we performed simulation with changing r_i/r_o and Rayleigh number *Ra*, and the Ekman, Prandtl, and magnetic Prandtl numbers are fixed to be *E* = 10^-3, *Pr* = 1.0, and *Pm* = 5.0, respectively.
Based on dipolarity, we limited the range of the sustained dynamo for all radius ratios. We found that the range for the strong dipole became narrower with a smaller inner core size. While the dependence of dipolarity on the Rayleigh number is similar at r_i/r_o = 0.25 and 0.35, the dipolar dominance becomes weaker with the smaller inner core. There were no strong dipolar dynamos but non-dipolar dynamos at 10.1 < *Ra* / *Rac* < 15.6, only at r_i/r_o = 0.15 cases. Our results indicate that changes in the radius ratio largely influence the dynamo regime and suggests that the non-dipolar geomagnetic field was possible when the inner core size is less than r_i/r_o = 0.15.

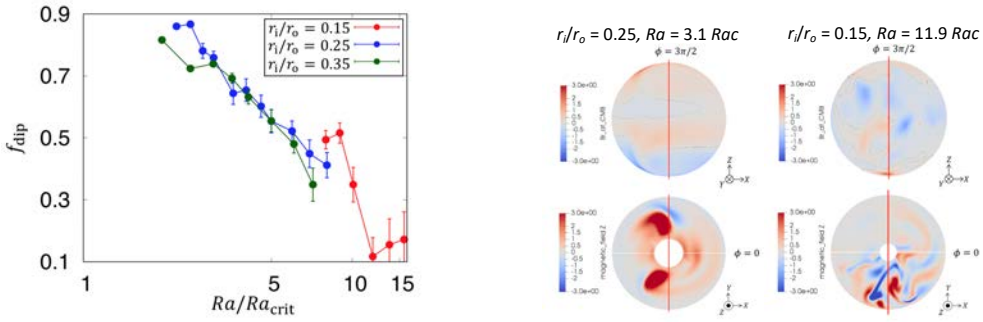

Dipolarity as a function of the ratio of Rayleigh number to the critical Rayleigh number (left). The generated magnetic field loses dipole component with increasing the Rayleigh number in all the inner core size cases. Spatial structure of the magnetic field is shown in the right panel. The result with the dipolar solution is shown in the left, and non-dipolar case is shown in the right. The radial magnetic field is plotted in the top panels and z-component of the magnetic field is plotted in the bottom. In the dipolar case, intense northward magnetic field is generated in the convection columns, but intense magnetic field is localized and have both directions in the non-dipolar case.

CIG Code(s): Calypso V.1.1

References

Nishida, Y., Y. Katoh, H. Matsui, M. Matsushima, T. Kera, and A. Kumamoto, Investigation of dipolar dominancy in geodynamo simulations with different inner core sizes, submitted to *J. of Geophys. Inter.*

Thermal Convection at Low Rayleigh Number

Grant Euen and Scott D. King
Virginia Tech

We use ASPECT to model 3-D thermal convection in a spherical shell in order to benchmark the results against legacy geodynamics codes. These models are based on the models computed using CitcomS by Zhong et al., 2008. The models are Boussinesq, incompressible, and have temperature-dependent viscosity. Each model has a larger change in viscosity, $\Delta\eta$, which causes an evolution through progressively more-complex mantle structures. The Rayleigh number for each of these models is low, on the order 10^3 to 10^5. We compute each of these models using two different grids at different levels of refinement: one grid is radially symmetric similar to the CitcomS grid used by Zhong et al., 2008, while the other is the default grid in ASPECT, which uses cells that vary in size based on radius. The default solution to the energy equation in ASPECT, entropy viscosity, is also compared with SUPG.

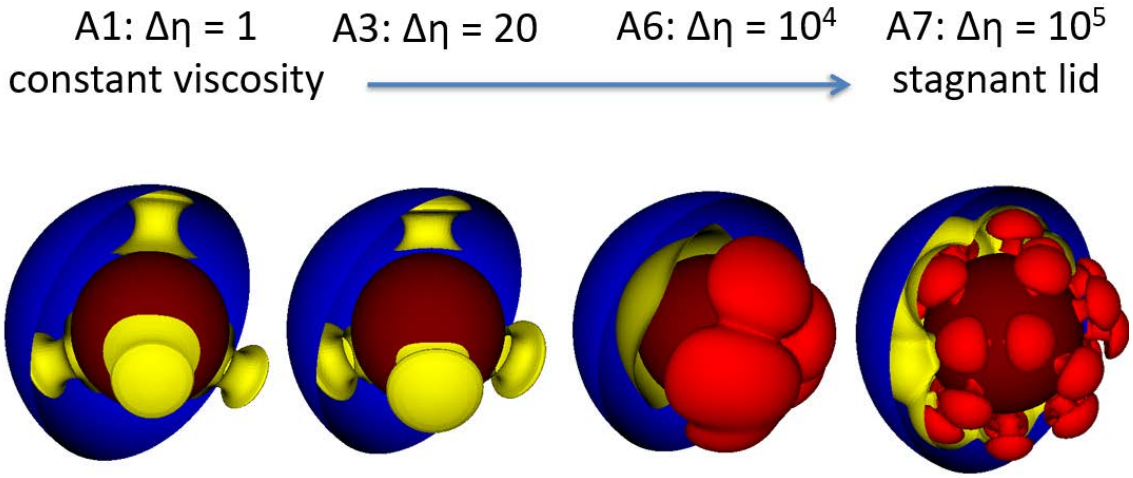

Images of isotherms taken from four models. These are based on cases A1, A3, A6, and A7 in Zhong et al., 2008. Images show upwellings of hot (yellow) and very hot (bright red) material with CMB (dark red) and surface (blue) shown.

Models are compared using root-mean-square velocity (V_{RMS}), average temperature, and the Nusselt number calculated at both the top and bottom of each model. We calculate agreement between the CitcomS and ASPECT results better than 1% for nearly all models. SUPG is also shown to give better agreement at lower grid refinement than entropy viscosity.

CIG Code(s): ASPECT and CitcomS

References

Euen, G. T. (2018). Studying 3D Spherical Shell Convection using ASPECT (Master's Thesis). Retrieved from https://vtechworks.lib.vt.edu/handle/10919/81621

Venus Resurfacing Constrained by Geoid and Topography

Scott D. King
Virginia Tech

When compared with Mars or the Moon, Venus has a small number of craters, indicating that the planet has been resurfaced in the last 250–750 Myr. The two candidate processes for this resurfacing are lavas from ~100 large volcanoes or the sinking of the cold, dense surface into the interior of Venus over a geologically short time period. In this work, a numerical model is used to study how the initial temperature and mechanical properties of the interior of Venus control resurfacing events. Comparing the predictions of the models with observations from Venus tests the numerical models. These predictions include the spatially variability of the gravity field, the overall shape of the planet, the center of mass of the planet, and whether there is enough energy within the core to generate a magnetic field. The numerical models demonstrate that the shape of the planet is not consistent with the cold sinking lithosphere process.

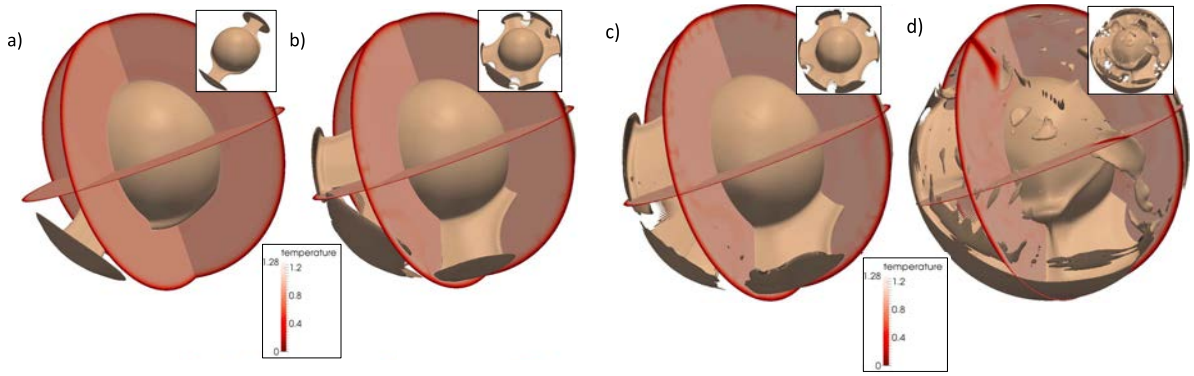

Representations of the potential temperature field (potential temperature isosurface as well as slices along equator and two north-south great circles) from Case 2 (l = 2, m = 1) initial perturbation pattern. (a) 222.2 Myr (2024 °C isosurface); (b) 352.1 Myr (2226 °C isosurface); (c) 425.5 Myr (2226 °C isosurface); (d) 556.3 Myr (2224 °C isosurface). The small inset figures at the lower left of each panel show the isosurface without the cross sections to better illustrate the pattern. All panels have the same orientation.

CIG Code(s): CitcomS

References

King, S. D. (2018). Venus resurfacing constrained by geoid and topography. *Journal of Geophysical Research: Planets*, *123*. https://doi.org/10.1002/ 2017JE005475

Calculation of viscoelastic seismic-cycle perturbations to the GPS velocity field for the USGS National Seismic Hazards Maps project

Elizabeth H. Hearn
Consulting Geophysicist, Portola Valley CA

I have developed seismic-cycle models using PyLith, to estimate viscoelastic perturbations to present-day GPS velocities due to past M>7.5 earthquakes on the San Andreas Fault (SAF). These models incorporate a range of ductile material distributions for the lower crust and upper mantle, including layers, layers plus a SAF shear zone, and 3D viscosities from the Southern California Earthquake Center (SCEC) community rheology model. Ductile materials are represented with Maxwell and/or Burgers viscoelastic rheologies, with parameter ranges constrained by geological, geophysical and laboratory studies.

For a range of parameter choices and ductile material distributions, these models yield significant perturbations to present-day surface velocities around the SAF (typically 6-10 mm/yr across the southern SAF, in a left-lateral sense). Because both the northern and southern SAF are near (or beyond) the end of their average recurrence intervals, present-day near-field strain rates are lower than average, biasing SAF slip rates inferred from GPS and elastic models to values below their long-term (Holocene) values. This problem may be addressed by subtracting modeled perturbations from the GPS field prior to inverting for slip rates. Modeled viscoelastic perturbations appear insensitive to viscosity heterogeneities unless they affect viscosities near a rupture. The models also suggest that present-day viscoelastic perturbations are fairly insensitive to timing of large earthquakes prior to the most recent event.

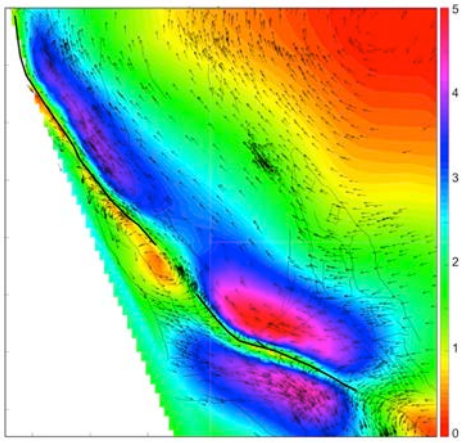

Present-day perturbations to the GPS velocity field in California due to large earthquakes on the northern and southern San Andreas Fault. Colors and arrows show velocity perturbation magnitudes (mm/yr) and orientations, respectively. Thick black lines show modeled northern and southern SAF ruptures. Since both faults are toward the end of (or beyond) their average recurrence intervals, strain rates around them are lower than the long- term average, and the perturbations show apparent left-lateral motion across the SAF.

CIG Code(s): PyLith 2.2.1

References

Pollitz, F.F. et al. (2021), Fault Slip Rates Contributed by Crustal Deformation Models to the 2023 Update to the National Seismic Hazard Model, Seis. Res. Lett., p. 1451.

Coupled flow and geomechanical modeling of deformation and seismicity induced by hydrocarbon and water extraction and CO2 and water injection

Birendra Jha
University of Southern California

Production and injection activities in faulted and stress-sensitive reservoirs can raise concerns of fault destabilization. Coupled numerical modeling of fluid flow and mechanical deformation in such reservoirs is an active area of research for the purpose of assessing the hazards of fault reactivation and induced seismicity during oil production, gas production, water extraction, wastewater disposal, geologic CO2 sequestration, and hydraulic fracturing. We use PyLith to perform coupled flow and geomechanical modeling of deformation caused by fluid extraction and injection in sedimentary basins. In 2014, we extended PyLith by coupling it with our multiphase flow simulator to perform these simulations. However, use of infinitesimal deformation models in long-term fluid withdrawal cases can predict inaccurate stresses and, therefore, inaccurate onset, magnitude, and duration of the fault slip events. To address this, we recently extended PyLith's finite strain deformation capability by coupling it with fluid flow and poroplasticity (Zhao and Jha, J. Comput. Phys. 2021).

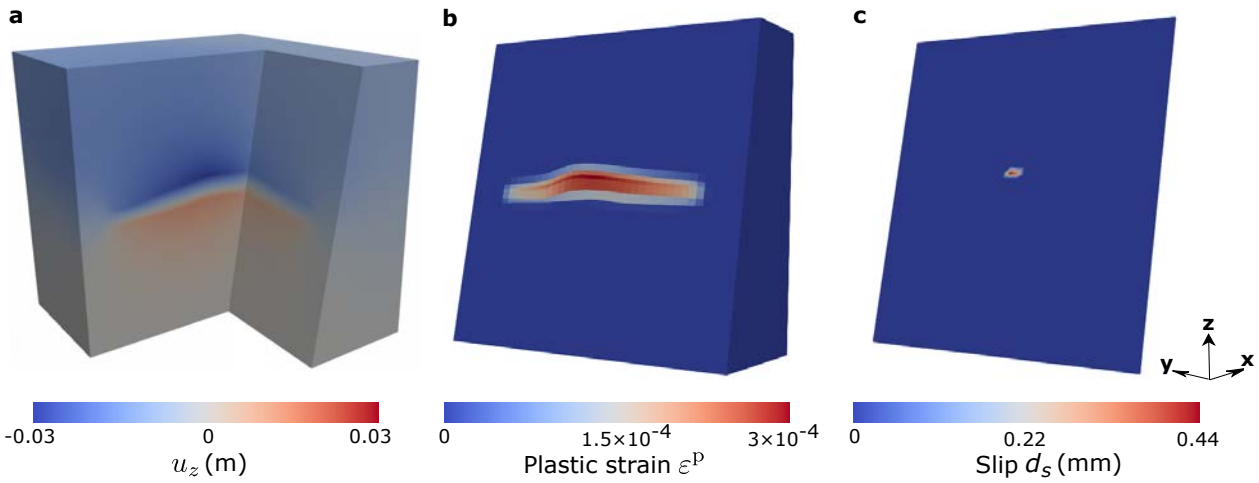

3D fields of (a) vertical displacement, (b) plastic strain magnitude in the footwall block, and (c) slip magnitude on the fault surface at day 850. (a) shows a cut-away view of the uz field using a slice along the fault surface and a y = 1000 m slice. (Zhao and Jha, J. Comput. Phys. 2021).

CIG Code(s): PyLith

References:

Zhao, X. and B. Jha, A new coupled multiphase flow-finite strain deformation-fault slip framework for induced seismicity, J. Computational Physics, 433, doi: 10.1016/j.jcp.2021.110178

Accounting for uncertain 3-D elastic structure in fault slip estimates

Théa Ragon and Mark Simons
Seismological Laboratory, Caltech

Earthquake source estimates are affected by many types of uncertainties. While observational errors are often accounted for, epistemic uncertainties, which stem from our simplified description of the Earth's interior, are usually neglected. In particular, 3-D variations in crustal properties are rarely considered. Here, we use PyLith to investigate, and account for, the impact of epistemic uncertainties related to 3-D variations of the mechanical properties of the crust. We combine a perturbation approach and a Bayesian sampling procedure, as applied to synthetic geodetic data generated from 2-D and 3-D finite-fault models. We show that accounting for uncertainties in crustal structure systematically increases the reliability of source estimates.

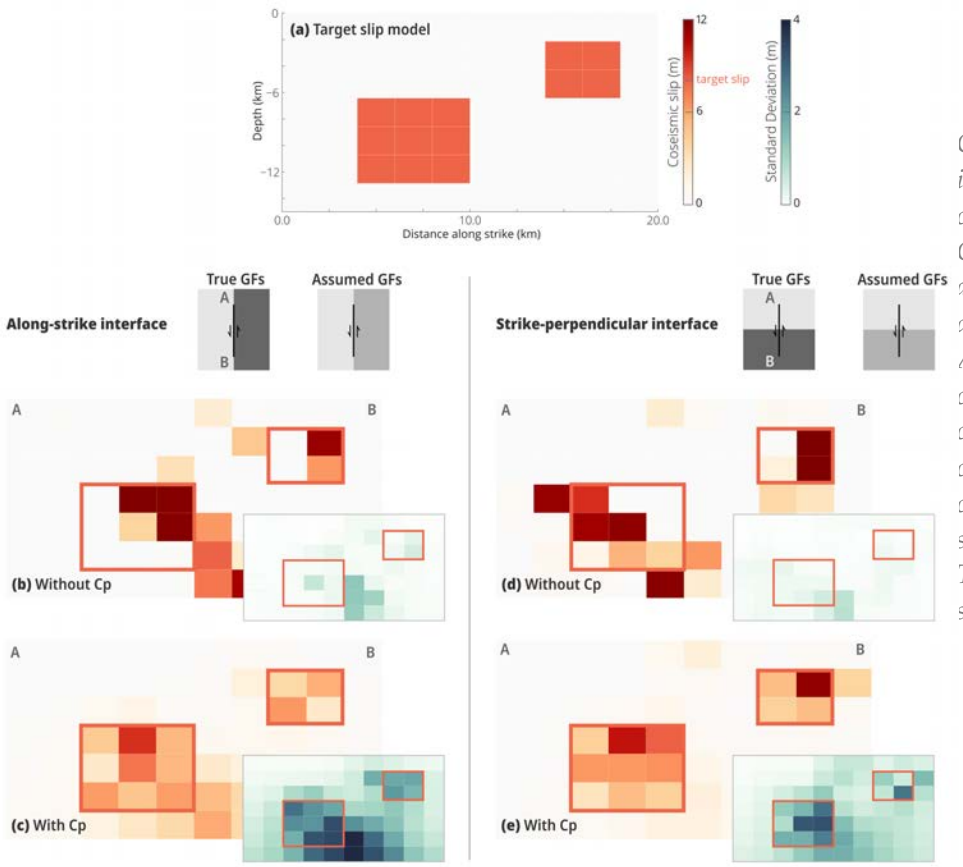

Comparison of slip models inferred assuming wrong crustal properties (or Green's Functions, GFs), accounting or neglecting derived uncertainties (Cp). Assumed crustal complexities are more compliant than the complexities used to compute the synthetic surface displacement. Target slip is purely strike-slip.

CIG Code(s): PyLith

References

Théa Ragon, Mark Simons, Accounting for uncertain 3-D elastic structure in fault slip estimates, *Geophysical Journal International*, Volume 224, Issue 2, February 2021, Pages 1404–1421.

Testing constitutive laws for the evolution of off-fault deformation over the earthquake cycle

Alba M. Rodriguez Padilla and Michael E. Oskin
University of California, Davis

A growing body of geologic and geodetic observations, including long-wavelength deformation around faults, steep slip gradients at step-overs, and the shallow slip deficit, requires stress relaxation by a distributed failure mechanism in the upper crust. Neglecting stress dissipation by off-fault deformation restricts the ability of earthquake-cycle models to simulate fault interaction and hampers the comparison of geodetic block models with long-term deformation. We add constraints to a constitutive law for off-fault deformation by modeling observations of fault-tip folding collected at coseismic, postseismic, and geologic timescales from locations spanning a variety of strain rates and lithologies, using open-access finite element code PyLith. This project will provide a constitutive law that accounts for stress dissipation by off-fault deformation for the next generation of geodynamic and earthquake-cycle models to incorporate, link coseismic strains to long-term crustal deformation, and guide future radar observations of the partitioning of seismic and aseismic deformation over the earthquake cycle.

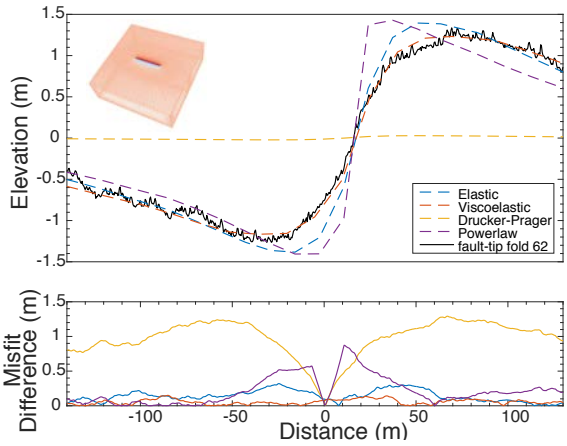

Preliminary models showing the fits different constitutive laws provide for off-fault deformation measured with lidar data from the Volcanic Tablelands. The mesh is generated based on the measured fault geometry from the lidar data and slip is imposed following the cumulative distribution measured from the lidar data.

CIG Code(s): PyLith

Acknowledgements: The modeling aspect of this project was started during the 2019 Crustal Deformation Modeling Workshop. Interactions with the developers and user community of PyLith through the online forum assisted in the development and refinement of the models.

References

Rodriguez Padilla, A.M. and Oskin, Michael E., Relaxation of earthquake stress via time-dependent off-fault deformation. In prep to be submitted to Nature Geoscience.

Determining the mechanics of joint San Andreas-San Jacinto earthquakes through Cajon Pass

Alba M. Rodriguez Padilla and Michael E. Oskin
University of California, Davis

Large, multi-fault earthquakes increase the threat of strong ground-shaking and reshape event probabilities across a system of faults. Fault junctions act as conditional barriers, or earthquake gates, that stop most earthquakes but permit junction-spanning events when stress conditions are favorable. Constraining the physical conditions that favor multi-fault earthquakes requires information on the frequency of isolated events versus events that activate faults through the junction. Measuring this frequency is challenging because dating uncertainties limit correlation of paleoseismic events at different faults, requiring a direct approach to measuring rupture through an earthquake gate. We show through documentation and modeling of secondary fault slip that co-rupture of the San Andreas and San Jacinto faults through the Cajon Pass earthquake gate occurred at least three times in the past 2000 years, most recently in the historic 1812 earthquake. Using a suite of numerical models in PyLith, we show that gate-breaching events have in common that they taper steeply and halt abruptly as they transfer slip between faults.

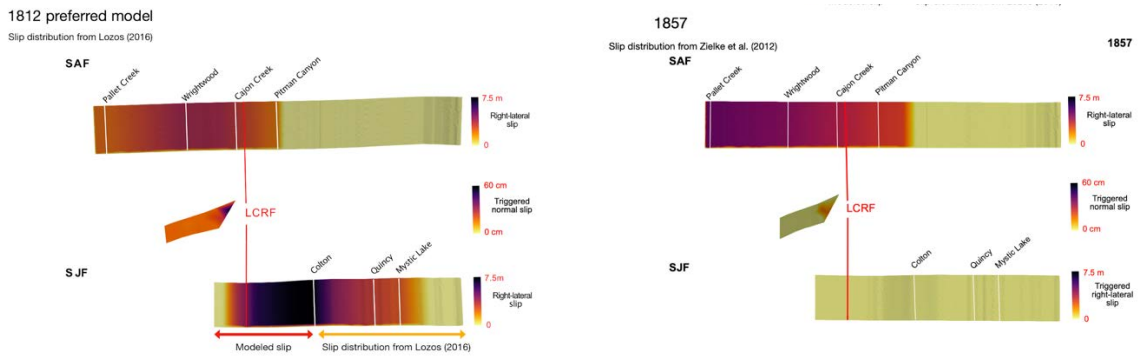

Slip models for the 1812 and 1857 earthquakes through Cajon Pass. Top: Preferred slip model for the 1812 event. Right-lateral slip imposed on the San Jacinto and the San Andreas is based on the final slip distributions in the preferred model in Lozos (2016). Slip north of the Colton paleoseismic site on the San Jacinto fault is based on the model that triggers the amount of slip measured in the LCRF trench from a suite of thirty tests. Bottom: 1857 event model based on the slip distributions in Zielke et al. (2012).

CIG Code(s): PyLith

Acknowledgements: The modeling aspect of this project was started during the 2019 Crustal Deformation Modeling Workshop. Interactions with the developers and user community of PyLith through the online forum assisted in the development and refinement of the models.

References

Rodriguez Padilla, A.M., Oskin, M. E., Rockwell, T. K., Delusina, I., and Singleton, D. M., Frequent Joint Earthquake Rupture of the San Andreas and San Jacinto Faults. Submitted to Nature Geoscience.

Full-wave numerical simulation of wave propagation in oceanic environments

Paul Cristini[1], Nathalie Favretto-Cristini[1], Vadim Monteiller[1] and Alexis Bottero[2]
[1]Laboratoire de Mécanique et d'Acoustique, Marseille, France, [2]Scripps Institution of Oceanography, San Diego, USA

The full-wave numerical simulation of acoustic wave propagation in the ocean is still a challenging problem due to the huge amount of computational resources which is required to simulate in-situ experiments that are commonly performed in underwater acoustics. Even if it's challenging, the availability of accurate results is crucial, and we started using SPECEFM for several applications where the use of a spectral-element has allowed us to obtain several new results, which gave us new insights into the physics of wave propagation. As an illustration, we show some results from the study of the impact of the explosion of unexploded ordnances in shallow water and from the study of the mechanism of generation and conversion of T waves at slopes.

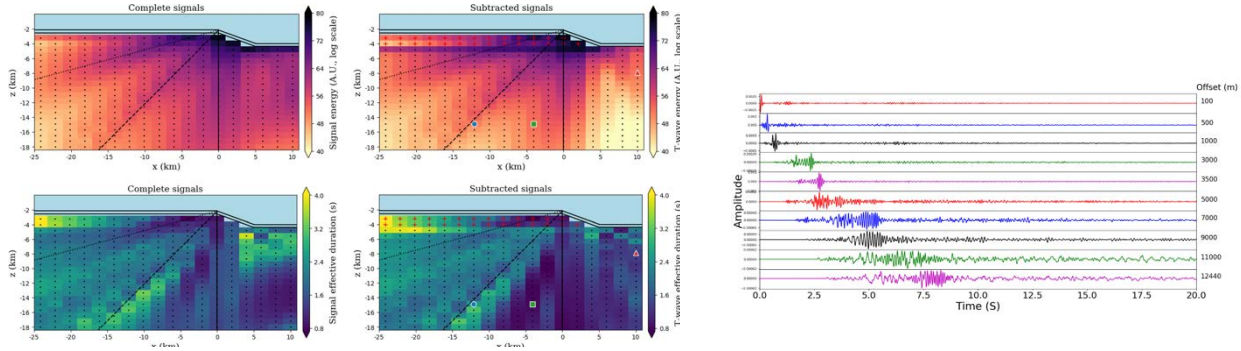

(left) Efficiency and time duration of slope converted T wave signals (right). Time signal evolution with distance to an explosive source in shallow water.

CIG Code(s): SPECFEM2D and SPECFEM3D

Acknowledgements: This paper was supported by The French National Research Agency (ANR) and co-funded by DGA (French Ministry of Defense Procurement Agency) ANR-15-ASTR-0001 POSA. The Ph.D. grant of Alexis Bottero was awarded by ENS Cachan, France.

References

Favretto-Cristini N. et al. (2021) Assessment of risks induced by counter-mining unexploded large-charge historical ordnance in a shallow water environment: Part 1. Real case study. IEEE Journal of Oceanic Engineering, in revision.

Favretto-Cristini N. et al. (2021) Assessment of risks induced by counter-mining unexploded large-charge historical ordnance in a shallow water environment: Part 2. Modeling of seismo-acoustic wave propagation. IEEE Journal of Oceanic Engineering, in revision

Bottero, A., Cristini, P., Komatitsch, D. (2020) On the Influence of Slopes, Source, Seabed and Water Column Properties on T Waves: Generation at Shore. Pure and Applied Geophysics 177, 5695–5711.

Preconditioned BFGS-based Full-Waveform Inversion & Uncertainty Estimation

Qiancheng Liu, Stephen Beller, Wenjie Lei, Daniel Peter, and Jeroen Tromp
Princeton University

Full Waveform Inversion (FWI) plays a vital role in reconstructing geophysical structures. The Uncertainty Estimation regarding the inversion results is equally important but has been missing out in most of the current geophysical inversions. Mathematically, uncertainty estimation is involved with the inverse Hessian (or the posterior covariance matrix), which is prohibitive in computation and storage for practical geophysical FWI problems. L-BFGS populates as the most efficient Gauss-Newton method; however, in this study, we empower it with the new possibility of accessing the inverse Hessian for uncertainty estimation in FWI. To facilitate the inverse-Hessian retrieval, we put together BFGS (essentially, full-history LBFGS) with randomized singular value decomposition towards a low-rank approximation of the Hessian inverse. That the rank number equals the number of iterations makes this solution efficient and memory-affordable even for large-scale inversions. Also, based on the adjoint method, we formulate different diagonal Hessian initials as preconditioners and compare their performances in elastic FWI. We highlight our methods with the elastic Marmousi benchmark, demonstrating the applicability of preconditioned BFGS in large-scale FWI and uncertainty estimation.

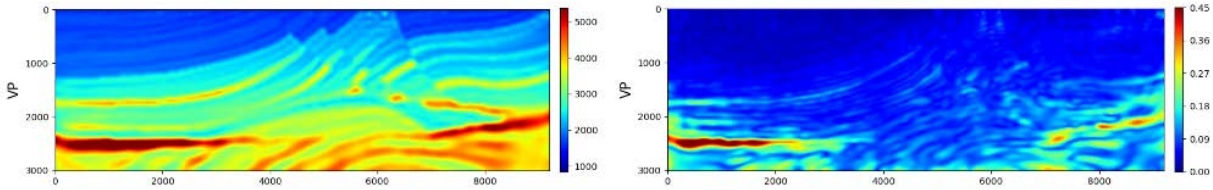

Images of the inverted P-wave Marmousi velocity result (left) and its uncertainty estimation map (right). The right map shows strong values for the model spaces with high uncertainties.

We see from the above figure the inverted P-wave velocity result and its uncertainty estimation map for the Marmousi benchmark. The uncertainty map makes sense because the sources and receivers are deployed on the earth surface of the model. It also shows that the uncertainty distributions can be quite structure dependent. For those complex ones with high velocities, they tend to have high uncertainties.

CIG Code(s): SPECFEM2D

References

Liu, Q., Beller, S., Lei, W., Peter, D and J. Tromp, Preconditioned BFGS-based elastic Full-Waveform Inversion and Uncertainty Estimation: Geophysical Journal International, Submitted.

Elastic Full Waveform Inversion of VSP Data from a Complex Anticline in Northern Iraq

Zhaolun Liu[1], Jürgen Hoffmann[2], Frederik J. Simons[1], and Jeroen Tromp[1]
[1]Princeton University, [2]DNO ASA

We demonstrate an application of isotropic elastic Full-Wave- form Inversion (FWI) to a field data set of Vertical Seismic Profiles (VSP) from a structurally complex narrow anticline in Northern Iraq. A practical elastic FWI workflow is developed to invert offset VSP seismic data. Synthetic tests indicate that this approach can give accurate wave speed updates for the target anticlinal structure. We use inverted wave speed models to perform elastic Reverse-Time Migration (RTM) of the data. The RTM results show that the shear wave speed (VS) image has a higher resolution than the compressional speed (VP) image for the target structure, owing to the presence of interpretable P-to-S converted waves. The results of the field test show that elastic FWI produces elastic models from which we obtain clear VS images of the thrust fault of interest.

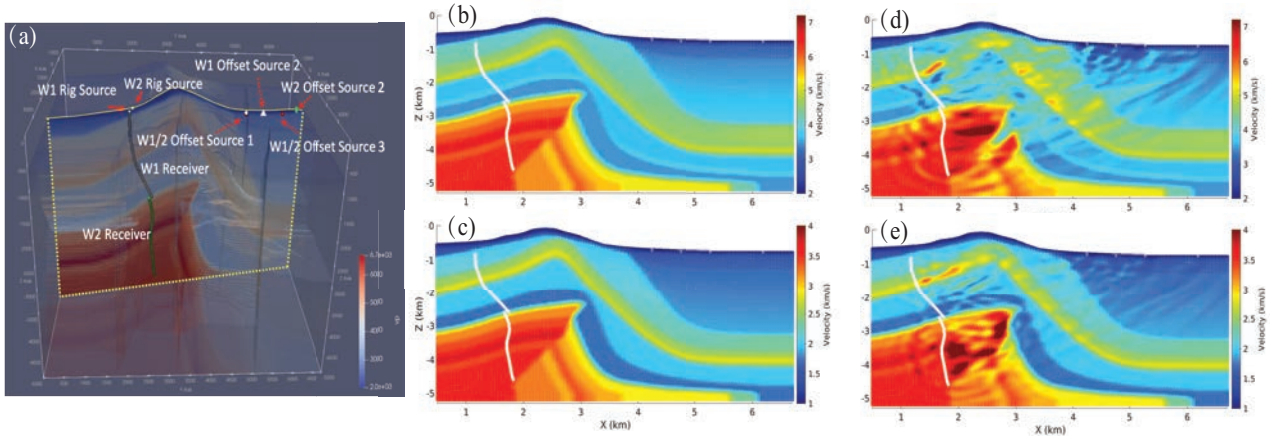

(a) A 2D wave speed slice in a 3D P-wave speed model; (b) and (c) are the initial Vp and Vs models; (d) and (c) are the inverted Vp and Vs models by elastic FWI.

CIG Code(s): SPECFEM2D, SPECFEM3D

Acknowledgements: DNO ASA, Norway; The Princeton Institute for Computational Science and Engineering (PICSciE), USA.

References

Liu, Z., J. Hoffmann, F. J. Simons, and J. Tromp, Elastic full waveform inversion of VSP data from a complex anticline in northern Iraq, submitted to SEG Technical Program Expanded Abstracts 2021

Merging Multiscale Models Improves Regional Seismic Wavefield Predictions near the Southern San Andreas Fault

Rasheed Ajala and Patricia Persaud
Louisiana State University

A potential seismic hazard facing Southern California is a large-magnitude earthquake from a San Andreas fault rupture with energy propagating into the densely populated greater Los Angeles area. To predict the expected ground-shaking from such an event accurately, researchers have put significant effort into developing seismic velocity models for the area, such as the Southern California Earthquake Center (SCEC) CVM-S 4.26 and CVM-H 15.1 community models. The goal is to utilize physics-based seismic hazard analysis to help Southern Californians prepare. Using a technique for generalizing the definition of window functions to higher dimensions with arbitrary support, we smoothly embed high-resolution basin-scale models developed using active source data into the SCEC community models. The community and hybrid Earth models are validated at low frequencies with medium magnitude earthquakes using SPECFEM3D. The hybrid Earth model provides better ground motion predictions than the SCEC community models, showing that one can readily use the method of embedding detailed local models to improve regional Earth models.

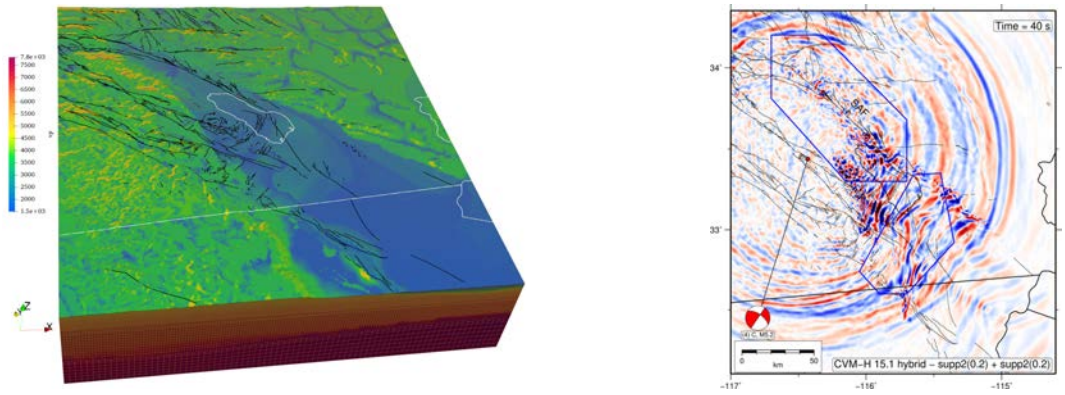

Salton Trough mesh generated with SPECFEM3D internal meshing program populated with crustal and upper mantle P wave velocities from a CVM-H 15.1 hybrid Earth model (left) and the wavefield snapshot showing vertical ground motion velocities from a medium magnitude earthquake that initiated in the San Jacinto fault zone (right). One can identify the S wavefront and sedimentary basin amplification.

CIG Code(s): SPECFEM3D

Acknowledgements: LSU high performance computing center for providing CPU hours on the supercomputers.

References

Ajala, R. and P. Persaud, Merging Multiscale Models Improves Regional Seismic Wavefield Predictions near the Southern San Andreas Fault, Journal of Geophysical Research: Solid Earth, In Revision, April 2021.

The Rupture Dynamics of Very Large Earthquakes

Jean-Paul Ampuero and Huihui Weng
Université Côte d'Azur, France

The largest earthquakes feature ruptures with large length-to-width ratio: once they span the whole seismogenic depth, they propagate horizontally. This geometrical constraint changes fundamentally the scaling behavior of earthquake energy, but is not accounted for by classical rupture models. We thus developed the fracture mechanics theory of elongated ruptures, which sheds light on what controls rupture arrest and rupture speed. For instance, it explains how earthquakes in oblique-slip faults can run at speeds previously thought to be energetically forbidden. These theoretical developments were motivated and validated by 3D dynamic rupture simulations on very large faults, using the spectral element method.

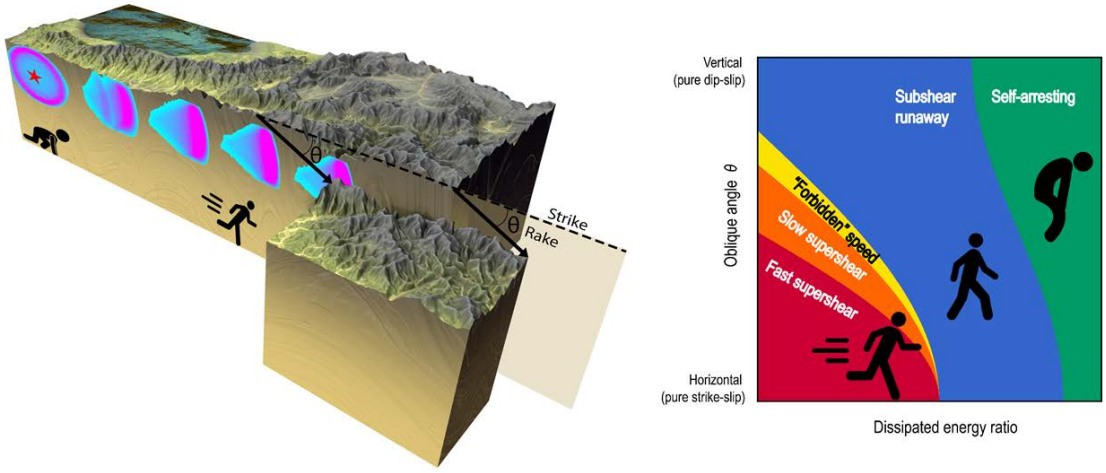

(Left) A large earthquake rupture with limited depth and oblique slip. Colors show the slip pulse sweeping along the fault, at five successive times, generated by numerical simulation. The red star is the hypocenter. (Right) Achievable steady-state rupture speeds as a function of the slip-obliqueness angle and the relative strength of the fault.

CIG Code: SPECFEM3D

Acknowledgements: In memory of Dimitri Komatitsch, whose pioneering work on the spectral element method in seismology and generous development of SPECFEM3D enabled a whole generation of computational seismology studies, including ours. This work was supported by the French government through the Investments in the Future project UCAJEDI (ANR-15-IDEX-01) managed by the French National Research Agency (ANR).

References

H. Weng and J. P. Ampuero (2020), Continuum of earthquake rupture speeds enabled by oblique slip, Nature Geo., 13, 817–821, doi:10.1038/s41561-020-00654-4.

H. Weng and J. P. Ampuero (2019), The dynamics of elongated earthquake ruptures, J. Geophys. Res., 124 (8), 8584-8610, doi: 10.1029/2019JB017684.

Efficient simulations of gravity and magnetic anomalies

Hom Nath Gharti[1], Jeroen Tromp[2], Stefano Zhampini[3]
[1]Queen's University, Kingston, ON, Canada, [2]Princeton University, NJ, USA, [3]King Abdullah University of Science and Technology, Thuwal, Saudi Arabia

Gravity and magnetic anomalies are analogous and are induced by density heterogeneities and magnetized objects, respectively, which can be measured on Earth's surface or in space. Both are governed by the unbounded Poisson/Laplace equation. We use the spectral-infinite-element method that combines the highly accurate spectral-element method with the mapped-infinite element method, which reproduces an unbounded domain accurately and efficiently. This combination is made possible by coupling Gauss-Legendre-Lobatto quadrature in spectralelements with Gauss-Radau quadrature in infinite elements along the infinite directions.

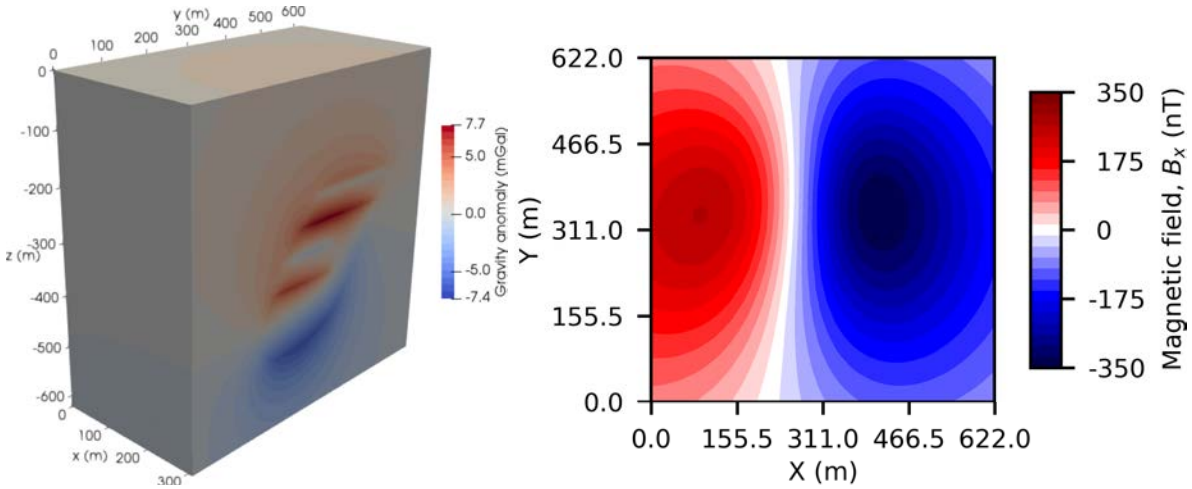

(Left) The computed gravity anomaly and (Right) The computed magnetic field for a 3D model of Pyhasalmi mine in Finland.

Our method has two distinct advantages over traditional methods. First, the higher-order discretization accurately renders complex heterogeneities. Second, since the computation time is independent of the number of observation points, the method is efficient for very large models.

CIG Code(s): SPECFEM3D

Acknowledgements: This research was partially supported by NSF grants 1644826 and 1550901.

References

Gharti, H. N. & Tromp, J., Spectral-infinite-element simulations of magnetic anomalies, *Geophysical Journal International*, **2019**, *217*, 1656-1667

Gharti, H. N.; Tromp, J. & Zampini, S., Spectral-infinite-element simulations of gravity anomalies, *Geophysical Journal International*, **2018**, *215*, 1098-1117

On-fault Geological Fingerprint of Earthquake Rupture Direction

Yoshihiro Kaneko[1] and Jesse Kearse[2]
[1]Kyoto University, Japan, [2]GNS Science, New Zealand

How earthquake ruptures evolve and propagate are major outstanding questions in seismology. Currently, we are unable to observe the details of earthquakes that occurred in the distant past, which limits our understanding to events recorded by modern technology. Here we propose a new method to uncover the rupture propagation direction of past large earthquakes, using geological features preserved on faults scarps. These features—called slickenlines—are scratch marks that form when two sides of a fault move past one another during an earthquake. Using spectral element simulations of spontaneous dynamic rupture, we develop a theoretical framework that links the geometry of slickenlines with rupture propagation direction for all types of faults. We then test our model using a global catalogue of surface-breaking earthquakes. Our results reveal a strong link between our model and the available data, providing a new way to uncover the rupture direction of large earthquakes that are not recorded by modern seismic instruments.

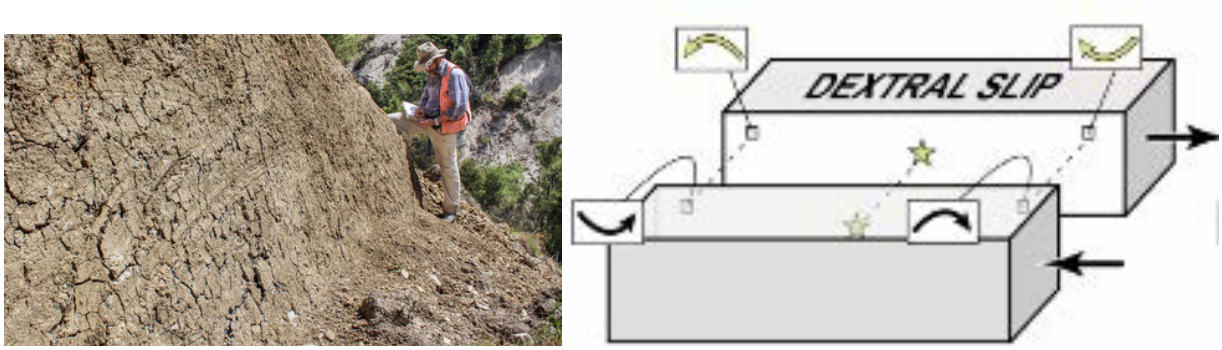

Kaikoura earthquake's curved slickenlines on the Kekerengu fault (left), and predicted shapes of slickenlines from dynamic rupture simulations(right). We find that slickenline convexity and rupture propagation directions in past large earthquakes are matched by the results of our models.

CIG Code(s): SPECFEM3D

Acknowledgements: This study was supported by Rutherford Discovery Fellowship from the Royal Society of New Zealand.

References

Kearse, J., Y. Kaneko, T. Little, and R.J. Van Dissen (2019). Curved slickenlines preserve direction of rupture propagation. *Geology*, 47 (9): 838–842, doi:10.1130/G46563.1

Kearse, J., and Y. Kaneko (2020). On-fault geological fingerprint of earthquake rupture direction, *Journal of Geophysical Research*, 125, doi:10.1029/2020JB019863

Testing the performance of a finite-frequency versus Ray Theory model using SPECFEM3D and stations of the Earthscope network.

Carene Larmat[1], Monica Maceira[2], Robert W. Porrit[3], David M. Higdon[4], Dale N. Anderson[1], Richard M. Allen[5]. [1]LANL, [2]OAK, [3]University of Texas, [4]Virginia Tech, [5]University of California, Berkeley

The Earthscope seismic network has produced a new generation of seismic models for North America with an unprecedented level of resolution. The publication of these new models is exciting as new features of North America plate and episodes of its history are unraveled, but it is also confusing when the findings are disparate.

We compare two models of western United States [1][2] coming from the Dynamic North America (DNA) seismic imaging effort [3] that only differ in the wave propagation method that was used for their inversion. Statistical analyses of S wave phase delay measurements, and comparison of waveform cross-correlation coefficients between FF and RT synthetics suggest that FF approaches to seismic imaging exhibit measurable improvement compared to RT for pronounced low-velocity anomalies such as the Yellowstone area.

We postulate that the use of a single low-frequency band for the DNA09-S model might have precluded larger differences between both seismic imaging methods, confirming the observation of [4] that the extra resolution of FF approaches originates from the use of multiple frequencies.

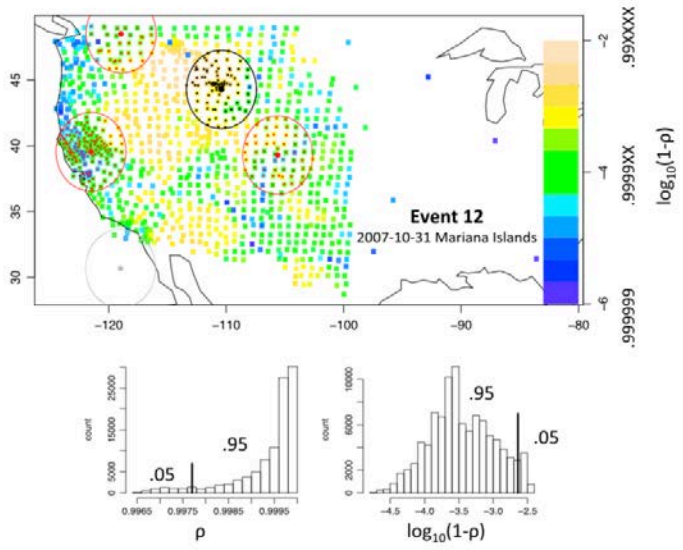

Permutation test for waveform coefficients for stations around Yellowstone for event 12 in our validation data set. (bottom) Histograms of cross correlations from 100,000 random locations indicate the Yellowstone region resides at about the 5th percentile (figure from [2])

CIG Code(s): SPECFEM3D

Acknowledgements: This research used resources provided by the Los Alamos National Laboratory Institutional Computing Program, which is supported by the U.S. Department of Energy National Nuclear Security Administration under Contract No. 89233218CNA000001. This is publication LA-UR-21-23660.

References

[1] Larmat, C. S., Maceira, M., Higdon, D. M., & Anderson, D. N. (2017). Joining statistics and geophysics for assessment and uncertainty quantification of three-dimensional seismic Earth models. *Statistical Analysis and Data Mining: the ASA Data Science Journal*, *10*(5), 277–289. http://doi.org/10.1002/sam.11353

[2] Maceira, M., Larmat, C. S., Porritt, R. W., Higdon, D. M., Rowe, C. A., & Allen, R. M. (2015). On the validation of seismic imaging methods: Finite frequency or ray theory? *Geophysical Research Letters*, *42*(2), 323–330. http://doi.org/10.1002/2014GL062571

[3] Obrebski, M., Allen, R. M., Xue, M., & Hung, S. H. (2010). Slab-plume interaction beneath the Pacific Northwest. *Geophysical Research Letters*, *37*(14), n/a–n/a. http://doi.org/10.1029/2010GL043489

[4] Mercerat, E. D., Nolet, G., & Zaroli, C. (2013). Cross-borehole tomography with correlation delay times. *Geophysics*, *79*(1), R1–R12. http://doi.org/10.1190/geo2013-0059.1

Imaging shear velocity and anisotropy of Alaskan lithosphere using ambient-noise adjoint tomography

Tianshi Liu[1], Bin He[1], Qinya Liu[1], Kai Wang[2], Yingjie Yang[2], Carl Tape[3] and Ping Tong[4]
[1]University of Toronto, [2]Macquarie University, [3]University of Fairbanks, [4]Nanyang Technological University

Multiple episodes of tectonic events have shaped the unique and complex geological structures in Alaska, and by mapping the subsurface velocity and anisotropy structures, seismic imaging can provide constraints on the tectonic evolution of the region. In this study, we use high-quality broadband seismic records over the entire Alaska from the recent deployment of USArray to image the shear velocity and anisotropy of the crust and uppermost mantle beneath Alaska. We collect all available continuous seismic data recorded from 2014 to 2020 at the broadband stations in Alaska, and follow the standard ambient noise data processing procedures extract the empirical Green's functions (EGF) between all available station pairs. Based on the adjoint method, we measure and minimize the frequency-dependent travel-time misfits between EGFs and the Green's functions simulated using the SPECFEM3D package to update the velocity model iteratively. We obtain a shear velocity and radial anisotropy model of the Alaskan crust and uppermost mantle from the surface down to ~70km depth.

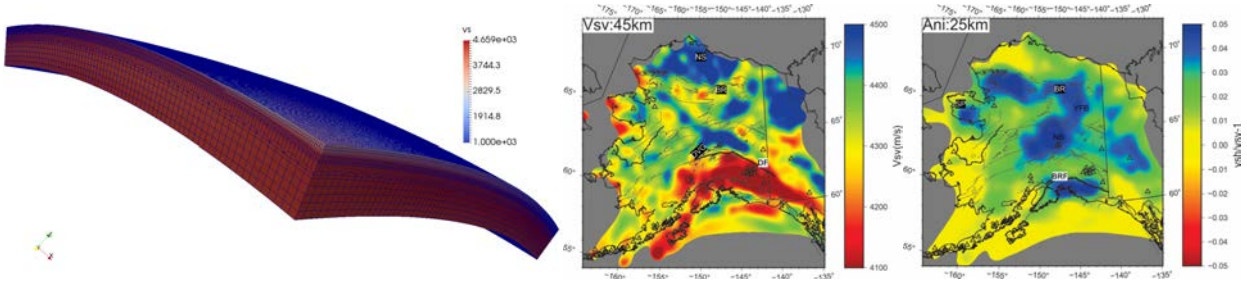

The mesh for our numerical simulation (left), taking into account the Earth's curvature, our shear-velocity model at 45km depth (center), and our radial anisotropy model at 25km depth (right)

CIG Code(s): SPECFEM3D

Acknowledgements: Computations were performed on the Niagara supercomputer at the SciNet HPC Consortium. SciNet is funded by: the Canada Foundation for Innovation; the Government of Ontario; Ontario Research Fund - Research Excellence; and the University of Toronto.

References:

Liu, T., K. Wang, C. Tape, B. He, Y. Yang, P. Tong and Q. Liu, Radial anisotropy of Alaskan lithosphere revealed by multi-component ambient-noise adjoint tomography, AGU Fall meeting 2020, S018-0004.

Crustal Deformation in Southern California Constrained by Radial Anisotropy from Ambient Noise Adjoint Tomography

Kai Wang[1,2], Qinya Liu[1], Yingjie Yang[2], Chengxin Jiang[3] and Vera Schulte-Pelkum[4]
[1]University of Toronto, [2]Macquarie University, [3]Harvard University and The Australian National University, [4]University of Colorado Boulder

The crust of Southern California has been shaped by complex tectonic processes through the evolution of the Pacific-North America plate boundary. The mechanisms of crustal deformation in this area are not fully understood. We investigate the deformation regime by the study of shear wave (Vs) radial anisotropy associated with mineral or structural orientations using the ambient noise adjoint tomography method based on 3D numerical simulations. Our work reveals pervasive positive radial anisotropy (Vsh > Vsv) in the crust and uppermost mantle, which is attributed to subhorizontal alignment of mica/amphibole foliation planes resulting from significant crustal extension. Interestingly, we also observe strong negative anisotropy (Vsh < Vsv) in the lower crust west of the San Andreas Fault that has not been reported before and is potentially created by either steeply dipping amphibole schists or subhorizontal alignment of plagioclase. The latter new mechanism highlights potentially complex CPO patterns resulting from different lithospheric mineralogy, as suggested by laboratory experiments on xenoliths from the region.

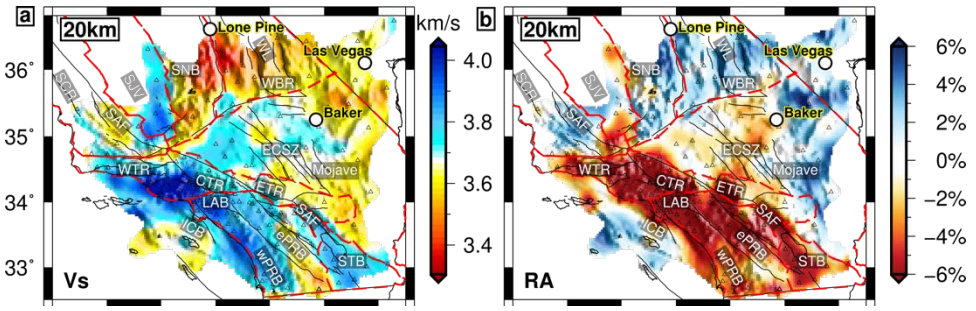

(a) The final shear-velocity (Vs) and (b) radial anisotropy (RA) at the depth of 20 km. Abbreviations of geological features can be found in the following published paper.

CIG Code(s): SPECFEM3D

Acknowledgements: Computations were performed on the Niagara supercomputer at the SciNet HPC Consortium. SciNet is funded by: the Canada Foundation for Innovation; the Government of Ontario; Ontario Research Fund - Research Excellence; and the University of Toronto.

References

Wang, K., C. Jiang, Y. Yang, V. Schulte-Pelkum, and Q. Liu. Crustal deformation in Southern California constrained by radial anisotropy from ambient noise adjoint tomography. Geophysical Research Letters 47, no. 12 (2020): e2020GL088580.

An Automated Workflow for Adjoint Tomography – Waveform Misfits and Synthetic Inversions for the North Island, New Zealand

Bryant Chow[1], Yoshihiro Kaneko[2,3], Carl Tape[4], Ryan Modrak[5], and John Townend[1]
[1]Victoria University of Wellington, [2]GNS Science, [3]Kyoto University, [4]University of Alaska Fairbanks, [5]Los Alamos National Laboratory

We develop and verify an automated workflow for full-waveform tomography based on spectral element and adjoint methods. We used the spectral element solver SPECFEM3D Cartesian to simulate 250 regional earthquakes and compared the resulting synthetics with recorded waveforms. We also performed a realistic synthetic inversion for 3-D checkerboard structure, analyzing model recovery, misfit reduction, and waveform improvement.

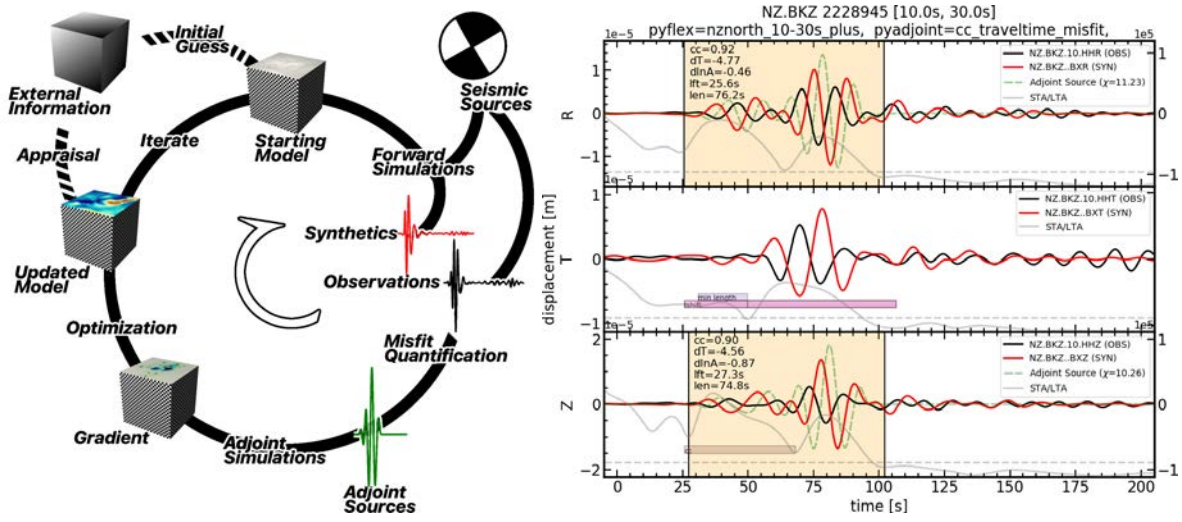

(Left) A diagram of our adjoint tomography workflow, built using the numerical solver SPECFEM3D Cartesian. (Right) Data-synthetic misfit assessment for a New Zealand earthquake. SPECFEM3D synthetics shown in red.

The relative ease of use and reliability of the workflow has led to an ongoing high-resolution (4–30 s), large-scale seismic inversion for the North Island, New Zealand. Updated models from such an inversion are expected to improve ground motion predictions, constrain complex velocity structures, and advance understanding of New Zealand tectonics.

CIG Code(s): SPECFEM3D Cartesian

References

Chow, B., Kaneko, Y., Tape, C., Modrak, R., & Townend, J. (2020). An automated workflow for adjoint tomography—waveform misfits and synthetic inversions for the North Island, New Zealand. Geophysical Journal International, 223(3), 1461-1480.

Diffracted Rayleigh waves from a deep Tunnel

Zhendong Zhang and Jeroen Tromp
Princeton University

We use a synthetic test to demonstrate the properties of transmitted and diffracted Rayleigh waves. The Vs model has a cavity (2 m by 2 m) in the model's center. The background wave speed model is a 1D inverted model (from the KGS team) from the DAY1 data. We generate common-shot-gathers (CSG) using the solver SPECFEM 3D Cartesian, in which the free-surface and topography are implemented accurately. A Ricker wavelet with a frequency band of 3—20 Hz is used in the simulation. Note that we only analyzed the vertical component of the data for simplicity. The Figure shows the predicted data from the Vs model without the cavity and their difference, respectively. The diffracted waves are too weak to be observed from the raw data (Figure a) directly. After subtracting the strong transmitted Rayleigh waves from the raw data, we can clearly identify the diffracted Rayleigh waves. The diffraction apexes indicate the cavity's horizontal location in the T-X domain (data domain). We use time-reversal imaging to project diffraction energy at their origins, i.e., candidate tunnels.

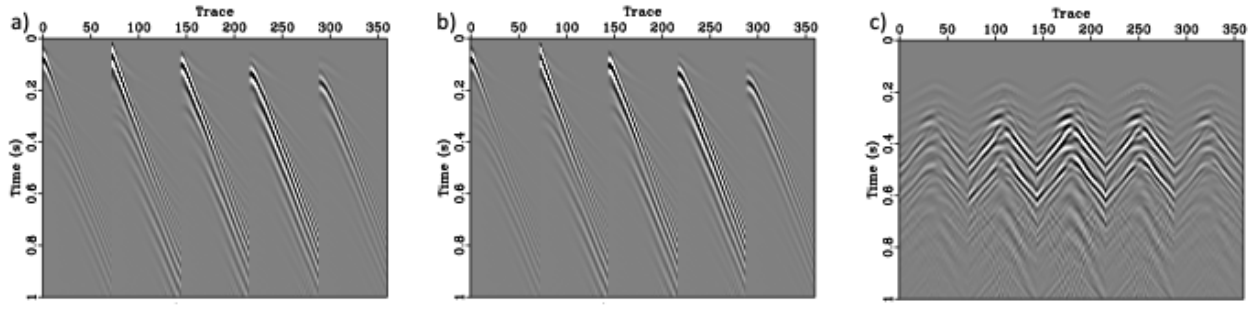

Predicted data and their difference. a) Predicted data from the actual Vs model with a tunnel. b) Predicted data from the actual Vs model only and c) the difference between two data sets. Diffracted Rayleigh waves are observed in c).

CIG Code(s): SPECFEM3D Cartesian

Regional Source Encoded Full Waveform Inversion

Congyue Cui, Etienne Bachmann, Wenjie Lei, Jeroen Tromp

We are experimenting with using source encoded full waveform inversion to obtain regional seismic structure. The data from each earthquake are encoded into a single "super" event which generates a "super" wavefield. Individual wavefields may be extracted from the super wavefield and used for kernel computations as in traditional inversions. By eliminating the need to compute kernels individually, the computational cost can be greatly reduced. Current synthetic results show a promising convergence rate. Only each iteration requires only 5-7 SPECFEM3D_GLOBE simulations and the model misfit reduced by about 65% after 20 iterations.

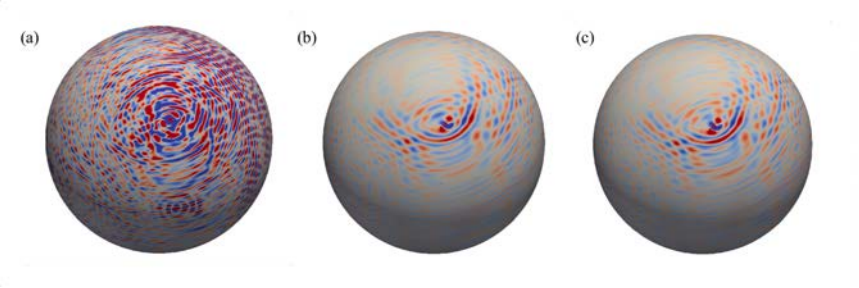

Images demonstrating the kernel deblending. (a) source encoded kernels computed with a "super" event which consists of 2 individual events, (b) individual event kernel deblended from (a), (c) individual event kernel computed without source encoding.

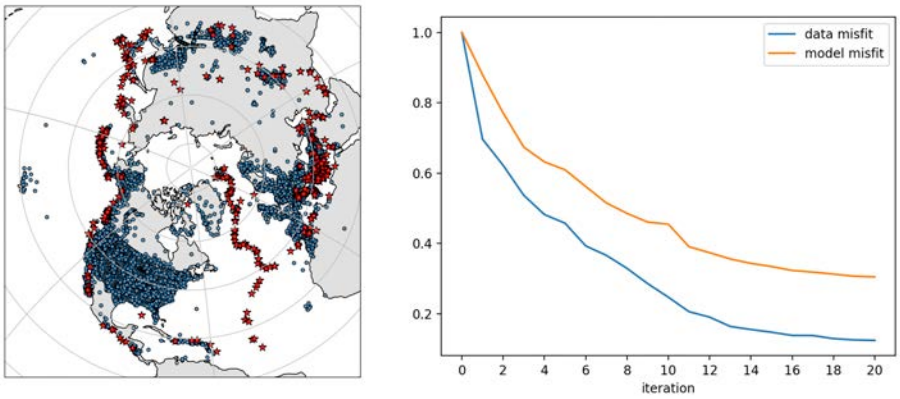

Research region (left) and misfit reduction over iterations in synthetic inversion (right).

CIG Code(s): SPECFEM3D_GLOBE

Acknowledgements: ORNL, NSF

References

Jeroen Tromp and Etienne Bachmann. Source encoding for adjoint tomography. Geophysical Journal International, 218(3):2019–2044, 2019.

Advancing our Understanding of the Earth using Seismic Tomography

Wenjie Lei and Jeroen Tromp
Princeton University, Princeton, NJ, USA

Seismic Tomography is a powerful tool to probe the Earth's interior via the inversion for the parameters governing seismic wave propagation. The resulting tomographic models reveal highly heterogeneous structures from the surface down to the core-mantle boundary (CMB), with a broad depth range that is difficult to cover in other disciplines. Yet, the translation of wave speeds and density information into knowledge of temperature and chemical composition remains a fundamental challenge, requiring interdisciplinary efforts to achieve convincing solutions. Further, the combination of seismological and mineralogical research facilitates mantle convection simulations.

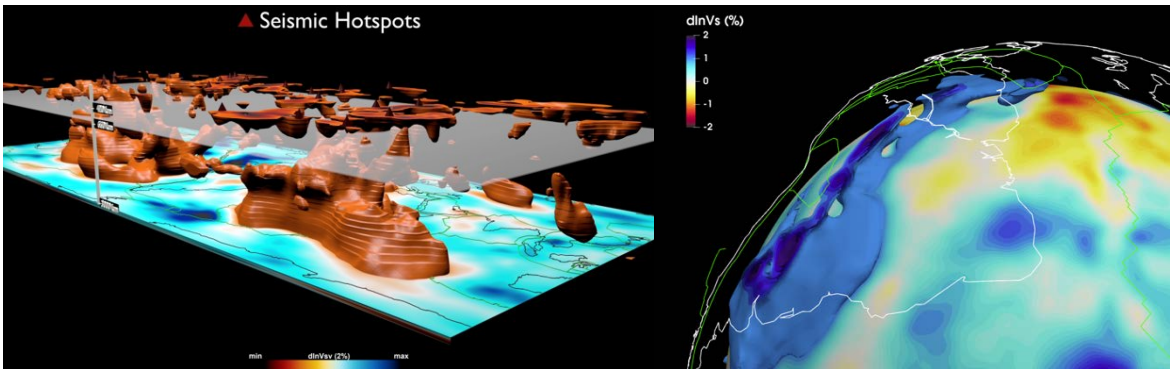

Iso-surface of low shear wave velocity anomaly in the mantle showing the structures of plumes; (Right) Iso-surface of high velocity anomaly in the upper mantle showing the subduction slabs in the South America.

In 2016, the first-generation of global adjoint tomography model, GLAD-M15 [15], was published, and the second-generation model, GLAD-M25 [16], just became available this year by harnessing the most powerful supercomputers, Titan and Summit [17], located at Oak Ridge National Laboratory.

CIG Code(s): SPECFEM3D_GLOBE

Acknowledgements: This research is supported by NSF grant 1644826.

References

Bozdağ, E., Peter, D., Lefebvre, M., Komatitsch, D., Tromp, J., Hill, J., ... & Pugmire, D. (2016). Global adjoint tomography: first-generation model. *Geophysical Journal International*, *207*(3), 1739-1766.

Lei, W., Ruan, Y., Bozdağ, E., Peter, D., Lefebvre, M., Komatitsch, D., ... & Pugmire, D. (2020). Global adjoint tomography—model GLAD-M25. *Geophysical Journal International*, *223*(1), 1-21.

Global Centroid Moment Tensor Inversion using 3D Green's Functions from Model GLAD-M25

Lucas Sawade, Wenjie Lei, Stephen Beller, Jeroen Tromp
Princeton University

For more than forty years the Global-CMT Project has provided earthquake centroid-moment tensors (GCMT) that are a staple for the seismological community. With the advent of global, high-resolution Earth models, the need for more accurate GCMTs became apparent. We use SPECFEM3D_GLOBE and the Global Adjoint Tomography Earth model GLAD-M25 for the computation of synthetics to invert seismic data for improved centroid moment tensors.

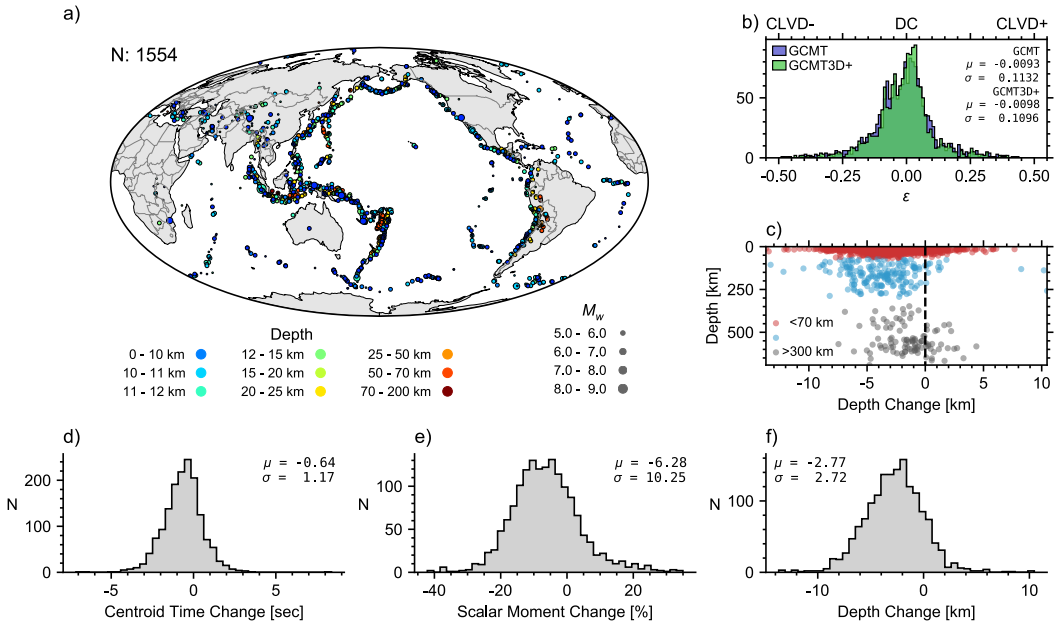

Preliminary results of 1554 inversions. For all plots μ and σ are the mean and standard deviation, respectively. a) Overview of events. b) Histograms of source type. c) Change of depth as a function of depth. d), e) and f) are histograms of changes in centroid time, scalar moment, and depth, respectively.

The new global centroid moment tensors (GCMT3D) show that GCMTs are on average ~3 km too deep, the centroid time ~1 s too late, and the scalar moment ~5% too high when first-order discontinuities, topography and bathymetry, self-gravitation, rotation, the ocean-load, and general heterogeneity of the Earth are taken into account.

CIG Code(s): SPECFEM3D_GLOBE

Acknowledgements: ORNL, PICSciE, NSF

References

Sawade, L., Lei, W., Beller, S. and J. Tromp, A New Database of Global Centroid Moment Tensor using 3D Green's Functions from Model GLAD-M25. Manuscript in preparation.

Convergence of Seismic Waves at the Antipode Generated by Impacts on Mars

Yuri Tamama and Jeroen Tromp
Princeton University (Junior Project)

When an impactor collides with a planet, the impactor's kinetic energy travels through the planet as seismic waves, which then merge at the antipode. We use SPECFEM3D_GLOBE to model impacts on Mars and study this antipodal seismic activity. The figures below show the results of an impact, oriented parallel to the vertical. Pictured are the displacement, velocity, stress, and strain in the crust and mantle under the antipode, at the top center of each panel. Consistent with Meschede et al., (2011), these parameters concentrate in vertical columns, shown in green, with values roughly an order of magnitude greater than its surroundings.

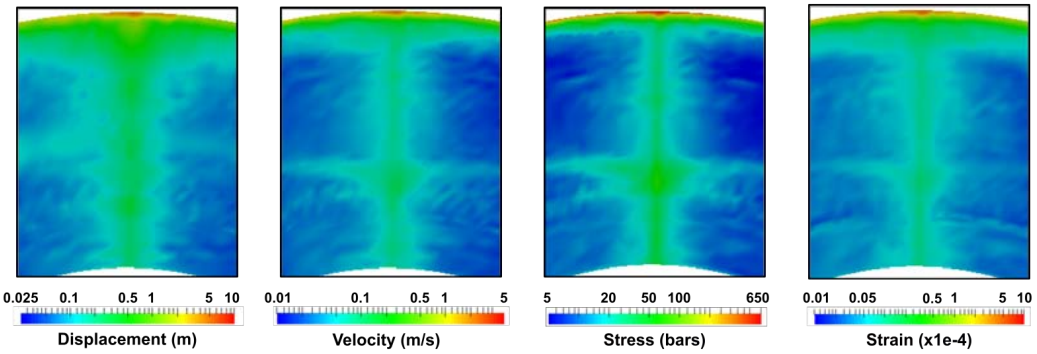

Maximum magnitudes of displacement, velocity, stress, and strain in the crust and mantle below the antipode (at the top), within one hour of a simulated vertical impact on Mars.

CIG Code(s): SPECFEM3D_GLOBE

References

Marinova, M. M., Aharonson, O., & Asphaug, E. (2011). Geophysical consequences of planetary-scale impacts into a Mars-like planet. *Icarus*, *211*(2), 960–985. https://doi.org/10.1016/j.icarus.2010.10.032

Meschede, M. A., Myhrvold, C. L., & Tromp, J. (2011). Antipodal focusing of seismic waves due to large meteorite impacts on Earth. *Geophysical Journal International*, *187*(1), 529–537. https://doi.org/10.1111/j.1365-246X.2011.05170.x

Peterson, J. E. (1978). *Antipodal effects of major basin-forming impacts on Mars*. https://www.lpi.usra.edu/meetings/lpsc1978/pdf/1307.pdf

Sohl, F., & Spohn, T. (1997). The interior structure of Mars: Implications from SNC meteorites. *Journal of Geophysical Research: Planets*, *102*(E1), 1613–1635. https://doi.org/10.1029/96JE03419

Williams, D. A., & Greeley, R. (1994). Assessment of Antipodal-Impact Terrains on Mars. *Icarus*, *110*(2), 196–202. https://doi.org/10.1006/icar.1994.1116

Exploring Basin Amplification Within the Reno Metropolitan Area Using a Magnitude 6.2 ShakeOut Scenario

Eric Eckert[1,2], Michelle Scalise[2], John N. Louie[2], and Kenneth D. Smith[2]
[1]Lawrence Berkeley National Laboratory (LBNL), [2]University of Nevada, Reno

The Reno Metropolitan area is subjected to significant seismic risk, especially from the Mount Rose fault system. We leveraged SW4, a physics-based wave-equation modeling tool, to develop the Reno ShakeOut Scenario. The Scenario is a 3D simulation for a potential magnitude 6.2 earthquake within the Mount Rose fault system in Reno, Nevada. Aggregating topographic, selected geotechnical measurements and gravimetry data produced a continuous 3D material property model for the urban basin. A Mw 6.2 Graves and Pitarka rupture drives the Reno ShakeOut Scenario, exploiting this material-property model to enhance our understanding of regional risk. The results indicate that there is a potential for widespread and variable ground shaking at Modified Mercalli Intensity (MMI) magnitudes between VII and VIII (very strong to severe ground shaking), with small areas achieving violent (IX) motions. Distributions of high shaking are controlled by proximity to the rupture, geotechnical shear-wave velocity, topography, and most significantly basin thickness. Significant basin amplification, over a factor of three between 1.0 and 3.125 Hz, seems to drive much of this variability. This information helps improve our understanding of regional risk by highlighting these significant basin effects and the local variability that is likely to occur with any large seismic event.

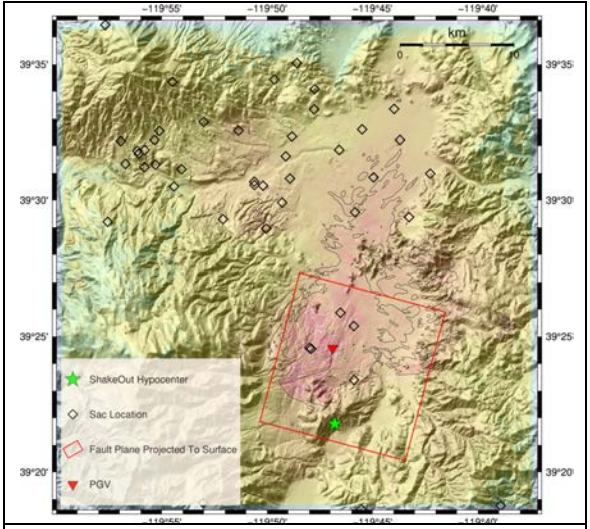

Shaking intensity map for the Reno M6.2 ShakeOut scenario, computed up to 3.125 Hz.

CIG Code(s): SW4 version 2.1

Acknowledgements: This material is based upon work supported by the U.S. Geological Survey under Grant No. G19AP00082. The DOE Critical Infrastructure Initiative provided time on the petascale CORI supercomputer at Lawrence Berkeley National Laboratory.

References

Eric Eckert, Michelle Scalise, John N. Louie, and Kenneth D. Smith, 2021 in revision, Exploring basin amplification within the Reno metropolitan area using a magnitude 6.2 ShakeOut scenario: submitted to *Bulletin of the Seismological Society of America*.

Effects of Energy Directionality on ReMi Analysis

Dustin Naphan[1], John N. Louie[1], Travis West[2], Aasha Pancha[3] and Bill Honjas[4]
[1]University of Nevada, Reno, [2]Washington Geological Survey, [3]Aurecon Group, Wellington, New Zealand, [4]Reno, Nevada

An obstacle shared by all passive surface wave analysis methods is the unknown source-receiver relationship, and possible adverse effects on apparent velocities. Particularly in the case of linear array geometry, the risk is that velocities will be overestimated if the direction of energy propagation is not approximately parallel to the array. Refraction Microtremor (ReMi) is a passive method that utilizes a linear array geometry. Our experimental approach to

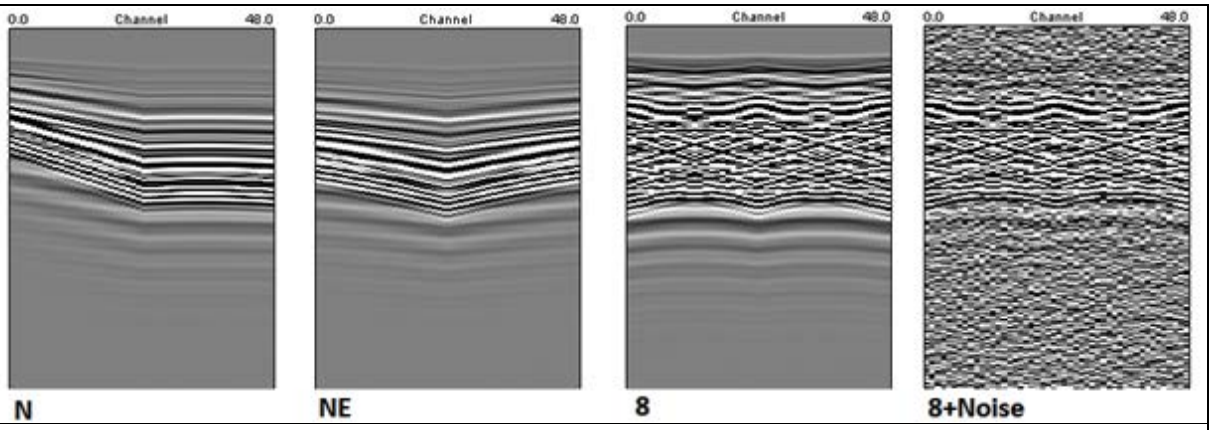

Synthetic data generated by the SW4 to 75 Hz from a 1D geotechnical model 0.5 km wide. From left to right the records are arranged as the source from the north (N), north-east (NE), 8 sources at once (8), and finally the case of all 8 sources with the addition of gaussian noise (8+Noise).

directional analysis makes use of a 2-D array configuration consisting of two linear arrays, arranged orthogonally in an "L" configuration. 3-D synthetic wave modeling using this configuration explores a variety of source-receiver orientations for directional effects. Based on the addition of omni-directional source energy to the worst-case synthetic scenario, the synthetic modeling helps decide the minimum proportion of energy necessary to have propagated in-line with the array to achieve an accurate result. This approach indicates such a proportion to be 15% of total rms amplitude, or 2.25% of the total energy.

CIG Code(s): SW4 version 1.18

Acknowledgements: Research partly supported by the U.S. Geological Survey (USGS), Department of the Interior, under USGS award number G16AP00109 to UNR; and G12AP20026, G14AP00020, and G15AP00055 to Optim.

References

Dustin Naphan, John N. Louie, Travis West, Aasha Pancha, and Bill Honjas, 2021 in revision, Effects of energy directionality on ReMi analysis: submitted to *Bulletin of the Seismological Society of America*, revised December 2019, 35 pp.

Improving Regional-Scale Simulation of Moderate Earthquakes by Combining Japanese Community Velocity Models with Interpolated Sub-Surface Velocity Profiles

Swasti Saxena, Ramin Motamed, and Keri L. Ryan
University of Nevada, Reno

Regional-scale simulation of a seismic event is highly dependent on its source, path, and site parameters. There are two widely used methods to model regional-scale simulations – one is to use a well-constrained community velocity model (CVM) which provides information about the deep and shallow crustal geology but severely lacks in low-velocity sub-surface structure. This method is insufficient to compute site-specific ground motions unless ground motions are adjusted using site amplification functions/factors. Another way is to create a horizontally layered model (HLM) by extending a single soil profile in two lateral dimensions. This method has its own drawbacks because it does not capture scattering of seismic waves passing through heterogenous media. To take the advantages of both the models, we combine the regional models with an interpolated sub-surface model computed from 1D soil profiles using a kriging algorithm (Hansen 2021). A comparison of ground motions simulated from different models with the recordings from an M3.5 earthquake show that the kriging model (KM) produces better amplitudes at the surface as well as better duration of motion due to wave scattering.

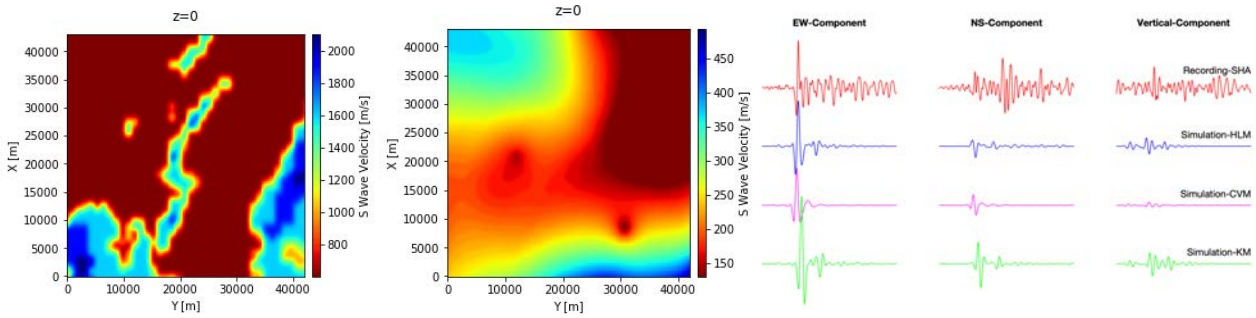

(Left) V_s map at the surface from J-SHIS, (Center) Vs map interpolated from several 1D V_s profiles-control points visible due lack of data in the simulation region, (Right) A comparison of simulations from the three models with data recorded at Service Hall Array (SHA), Kashiwazaki-Kariwa Nuclear Power Plant, Japan.

CIG Code(s): SW4 (Seismic Waves, 4th order)

Acknowledgements: We are grateful for the Department of Energy to fund this project under the NSR&D program and thank Los Alamos National Laboratory for sharing their HPC resources to carry out these regional-scale simulations.

References

Hansen, T.M. (2021). mGstat (https://github.com/cultpenguin/mGstat/releases/tag/1.0), GitHub. Retrieved May 10, 2020.

Petersson, N. Anders, & Sjogreen, Bjorn. (2017, November 20). geodynamics/sw4: SW4, version 2.01 (Version v2.01). Zenodo. http://doi.org/10.5281/zenodo.1063644.

Effect of Random 3D Correlated Velocity Perturbations on Numerical Modeling of Ground Motion from the Source Physics Experiment

Michelle Scalise[1], John N. Louie[1], Kenneth D. Smith[1], and Arben Pitarka[2]
[1]University of Nevada, Reno, [2]Lawrence Livermore National Laboratory (LLNL)

Explosions are traditionally discriminated from earthquakes using the relative amplitude of compressional and shear waves at regional and teleseismic distances, known as the P/S discriminant. The disparity is largely due to ground motion from small, shallow sources being significantly impacted by near-surface structural complexities. To understand the implications of wave propagation effects in generation of shear motion and P/S ratio during underground chemical explosions, we performed simulations of the Source Physics Experiment (SPE) chemical explosions using 1D and 3D velocity models of the Yucca Flat basin. All simulations used isotropic point sources in the frequency range 0-5 Hz. Comparisons of recorded and simulated waveforms for the SPE-5 explosion using 3D velocity models demonstrate that the shallow structure of the Yucca Flat basin contributes to generation of observed shear motion.

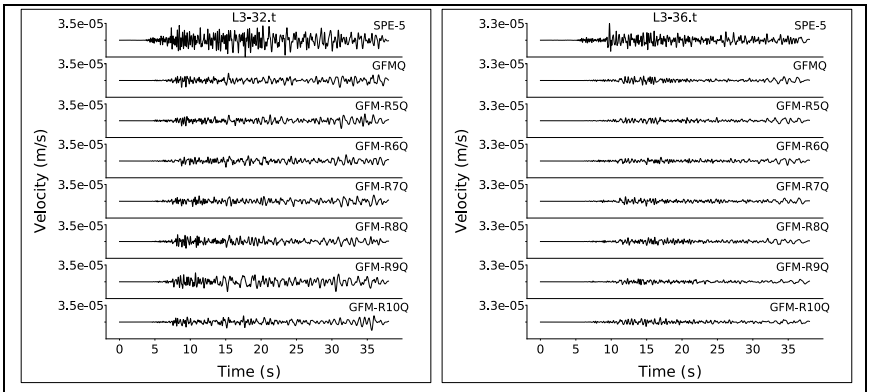

Recorded SPE-5 velocity data at L3-32.t and L3-36.t bandpass filtered from 0.5-5 Hz. Synthetic velocity waveforms at L3-32.t and L3_36.t computed in the 3D simulations convolved with a Mueller Murphy explosion source time function, amplitude scaled, and bandpass filtered from 0.5-5 Hz. L3-32 and L3-26 are located at the southern end of Yucca Flat basin.

The inclusion of 3D wave scattering, simulated by small scale velocity perturbations in the 3D model, improves the fit between the simulated and recorded waveforms. In addition, a relatively low intrinsic attenuation, combined with small scale velocity variations in our models, can confirm the observed wave trapping, and its effect on duration of coda waves and the spatial variation of P/S ratio at basin sites.

CIG Code(s): SW4 version 2.1

Acknowledgements: Simulations were performed on the Lassen cluster at Lawrence Livermore National Laboratory using Computing Grand Challenge allocation for Seismic and Acoustic Simulations.

References

M. Scalise, A. Pitarka, J. Louie, and K. D. Smith, 2021 in press, Effect of random 3D correlated velocity perturbations on numerical modeling of ground motion from the Source Physics Experiment: accepted to *Bulletin of the Seismological Society of America*, October 2020, 53 pp.

Sensitivity tests of detailed shear-wave velocity profiles to 95 m depth in 3D numerical simulations of wave propagation to 15 Hz frequency, Clark County, Nevada

L. Travis West[1], John N. Louie[2] and Satish Pullammanappallil[3]
[1]Washington Geological Survey, [2]University of Nevada, Reno, [3]Reno, Nevada

Including detailed velocity structure that better represents heterogeneous near-surface geology in 3D velocity models used deterministic simulations is an important step in accurately simulating ground motions at frequencies interesting to engineers (>10 Hz). In order to highlight site effects at higher frequencies attributed to small-scale, heterogeneous near-surface velocity structure, we perform 3D finite-difference simulations up to 15 Hz on 3D models that incorporate detailed velocity structure in the upper 95 m. We base the upper 95 m portion for both model types on the uniquely detailed and spatially dense 1D shear-wave-velocity-profiles (SWVPs) from the Clark County Parcel Map database for Las Vegas described by Pancha et al. in 2017. Fourier Spectral Ratio (FSR) results depict only slight variability in spectral amplification at the resonant frequency range of the Vs30-based models (1.6 to 3.6 Hz). However, above 4.6 Hz ground motions are being amplified on average by approximately 50% above the Vs30-based models, by the detailed model. As a corollary, this study demonstrates the use of finite-differencing numerical based methods to simulate ground motions at high frequencies, up to 15 Hz.

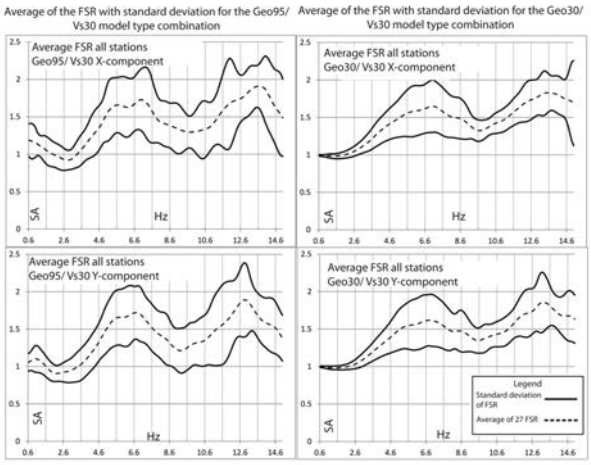

Average of the 27 FSR for each model combination (dashed line) with standard deviations (solid lines) of the 27 sites. The FSRs for Geo30/Vs30 combination (right column) depict little to no spectral amplification at the Vs30 resonance frequencies but both combinations consistently depict over 50% spectral amplification above 4.6 Hz.

CIG Code(s): SW4 version 1.18

Acknowledgements: The Clark County Parcel Map was developed by Optim and the Nevada Seismological Laboratory under contract with the Clark County Department of Development Services and the City of Henderson, Nevada.

References

L. T. West, Louie, J., Pullammanappallil, S., Sensitivity tests of detailed shear-wave velocity profiles to 95 m depth in 3D numerical simulations of wave propagation to 15 Hz frequency, Clark County, Nevada (paper 1127): *Proceedings of the 11th National Conference in Earthquake Engineering*, Earthquake Engineering Research Institute, Los Angeles, Calif., 5 pp.